AGH

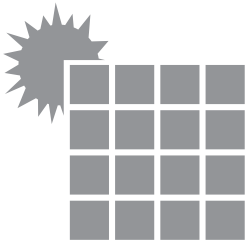

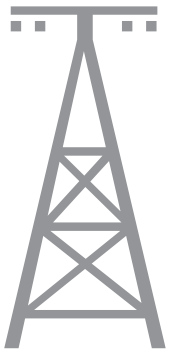

JOURNAL OF GEOTECHNOLOGY AND ENERGY

FORMERLY AGH DRILLING, OIL, GAS

2021, vol. 38, no. 1

AGH WYDAWNICTWA AGH

KRAKOW 2021

The "Journal of Geotechnology and Energy" (formerly "AGH Drilling, Oil, Gas") is a quarterly published by the Faculty of Drilling, Oil and Gas at the AGH University of Science and Technology, Krakow, Poland. Journal is an interdisciplinary, international, peer-reviewed, and open access journal. The articles published in JGE have been given a favorable opinion by the reviewers designated by the editorial board.

Editorial Team

Publisher

AGH University of Science and Technology Press

Linguistic corrector: *Aeddan Shaw*
Technical editor: *Kamila Zimnicka*
Desktop publishing: *Munda*
Cover design: *Paweł Sepielak*

Journal website: https://journals.agh.edu.pl/jge

Wydawnictwa AGH (AGH University of Science and Technology Press)
al. A. Mickiewicza 30, 30-059 Kraków
tel. 12 617 32 28, 12 636 40 38
e-mail: redakcja@wydawnictwoagh.pl
http://www.wydawnictwoagh.pl
http://www.wydawnictwo.agh.edu.pl

CONTENTS

Journal of Geotechnology and Energy | vol. 38 | no. 1 | 2021 | pp. 5–10

Chrystian Mazur

ORCID: 0000-0001-9777-8254
AGH University of Science and Technology in Krakow

SAFETY AND HEALTH HAZARDS DURING SERVICING WELLS: THE EXAMPLE OF SLICKLINE SERVICES

Date of submission:
26.05.2021

Date of acceptance:
7.06.2021

Date of publication:
31.07.2021

https://journals.agh.edu.pl/jge

Abstract: In the oil and gas industry there are many serious hazards. Possible aftereffects of accidents happening on wells producing gas or crude oil can have fatal consequences. Natural dangers such as high pressures, flammable and explosive fluids, H_2S content all make every project demanding and special care should be taken when planning works in harsh conditions. There are many precautions that could be done to ensure the long service life of the production wells and these can be achieved with slickline services. Slickline is usually a good first choice to conduct operations on live wells, and the potential risks during this work should be analysed since safety measures are crucial for both people and the environment. Only after assessing them correctly can work be done securely and in a timely manner.

Keywords: slickline, pressure control equipment, well servicing, oil and gas

1. Introduction

Nowadays the oil and gas industry, particularly the exploration and production branches, are starting to adapt to new market environments, with changes increasingly being made to make it both safer and more environmentally friendly. The long history of drilling has contributed to its safety but accidents still happen due to various reasons and their consequences are often significant. Accidents often affect only the economic aspects of the project, but sometimes they can affect the safety of people and the environment, thus it is crucial to prevent them from happening and minimize possible aftereffects.

The best known incident is probably the oil spill in Gulf of Mexico from the Deepwater Horizon platform, which happened on April 20th 2010. This accident caused 11 fatalities among the oil platform crew and severely impacted the marine and coastal environment. This blowout resulted in more than 110 000 km^2 of oil spill on the ocean surface and 2,100 km of shoreline being contaminated by hydrocarbons. This has negatively affected a wide range of organisms residing in contaminated habitats [1].

Serious accidents which have caused damage to the environment have also happened in Poland. An open blowout of reservoir fluid containing H_2S took place in Daszewo-1 wellsite near Karlino on 9th December 1980 during drilling. Fluid from the reservoir started to flow from the well and caught fire. Rescue operations took 33 days to contain the blowout. As a result of this blowout, an area in the radius of 600 m from the wellhead was degraded, 27 ha of soil was contaminated by hydrocarbons and the drilling rig was completely destroyed. However, after 30 years there are indicators that the environment was recultivated properly [2].

2. Hazards in the exploration and production industry

There are many hazards during drilling and servicing already producing wells. The most distinctive are probably hazards related to reservoirs: high pressures, flammable and explosive fluids, toxic fluids (mainly H_2S) and a risk of the reservoir fluid blowout. Geological conditions in Poland, particularly in the Polish Lowland, are unfavourable. From the abovementioned hazards, all occur at the same time.

The BMB (Barnówko-Mostno-Buszewo) field, is one of the mature fields with many deep wells drilled and it could be used as an example field in the Polish Lowlands. The BMB field produces both crude oil and natural gas. The reservoir pressure gradient was originally anomalously high, even 0.023 MPa/m, and there is also H_2S in the reservoir fluid produced. All these elements could be potentially harmful for people and for the environment [3].

Geological layers are heterogenous and their parameters can change in different places. This can mean that two identical wells could have different reservoir properties even though the wells are placed in the vicinity of one another. We can never be sure about exact parameters in the reservoir until the well is drilled. We could only use nearby wells as a reference and use geophysical methods to estimate them, but during the planning phase of the drilling project, all uncertainties should be taken into account.

Apart from natural hazards there is also a category of hazards associated with working with heavy equipment: heavy objects lifted to large heights, moving parts, high air and hydraulic pressures, electricity, and many others.

3. Well servicing

Well servicing is an important part of the life of the well. After completing the well, it starts production and through a long contact with a reservoir fluid, which could be corrosive, elements of the completion assembly start to deteriorate. Best practice shows that the condition of the well completion should be assessed regularly to ensure long service of the well.

Servicing wells is primarily conducted by coiled tubing services, wireline services (braided line and slickline), snubbing services or using a workover rig. In Poland, the first choice are primarily wireline services because the cost of their operation is significantly smaller than others.

Slickline is a part of the well servicing operations that are widely used, mainly being employed to obtain fluid samples from the wellbores, and measure pressure profiles in temporarily stopped production wells. The greatest benefits of slickline operations are: low cost of operations, an easy and quick mobilization, an ability to work on live and producing wells, short time of operations – wire could be pulled in and out safely with speeds exceeding 0.83 m/s (50 m/min).

4. Risks during servicing live wells

When servicing the live well, we have one less barrier to contain the reservoir pressure. During drilling, mud exerts hydrostatic pressure on the reservoir which stops reservoir fluid from flowing into the borehole and to

the surface. When working with a producing well, only there servoir fluid is in the completion string. It could be either gas or crude oil or a mixture of both. A reservoir fluid could be contaminated by H_2S and thus extremely toxic to people and it also could have significant pressure even on the surface. To prevent it from flowing out of the hole, pressure control equipment assembly is used. There are also hazards related to fire and explosion risk. When hydrocarbons make a mixture with air, they become combustible or can create an explosive atmosphere.

Before beginning a project, all hazards should be determined, especially natural hazards. Pressure control equipment should have pressure rating exceeding expected pressures increased by a risk factor. Moreover, if there is a possibility of H_2S occurrence, every piece of equipment should be able to cope with it.

Aggressive fluids could hasten the rate of corrosion, and weaken both elements of the pressure control equipment, tools and the wire in the wellbore during a lengthy exposure. It is crucial to control the rate of the corrosion of different elements of the tools and equipment and to clean them thoroughly and properly maintain them after exposure. Before the job, all equipment and tools should be visually inspected, particularly all elastomer O-rings and seals should be checked and changed if necessary.

In the presented Figure 1 there is a schematic of a typical pressure control assembly used during slickline operations on live wells. From the top, the first piece is a stuffing box, a part where the running or stationary wire is sealed. It consistsof a sheave to guide a wire and a series of packings which prevents reservoir fluid from leaking, and stuffing the box body. It could be also pressurized using hydraulic fluid to compress packings on the wire more tightly since packings will wear outduring long operations. The second is a liquid chamber connected to a pump located on the surface near the well with the check valve on the line. It enables liquid to be pumped to grease the running wire to minimize corrosion and drag on the stuffing box packings. The third section are lubricators, connected with quick union connections. Their length should be greater than the length of the whole tool string with some safety margin. When the operation assumes that some equipment or fish would be taken from the well the lubricator assembly length should be greater than the combined lengths of a tool string with a pulled object. On the lower part of the lubricator section there are ports with needle valves, they could be used to monitor pressure in a pressure control equipment or to bleed a pressure from it when the tool string is pulled out of the hole after operation. Number four is the blowout preventer, so called BOP, it functions as a valve to seal a wellbore from the surface and from the rest of the pressure control equipment. Depending on the type,it could be closed hydraulically and manually or only manually. It could close without anything between the rams or with the wire between them. A last part of the completion assembly is a flange adapter which connects pressure control equipment to the wellhead assembly. It contains a metal-metal seal to ensure tightness.

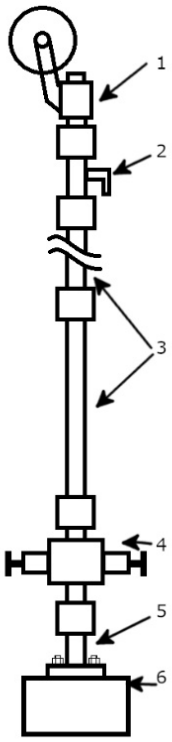

Fig. 1. Schematic of a typical pressure control equipment assembly during slickline operations:
1 – a stuffing box with a sheave, 2 – a liquid chamber,
3 – lubricators, 4 – a blowout preventer, 5 – a flange adapter,
6 – top of the wellhead

Another type of risk is a chance of the toolstring being stuck. In producing wells, there are many mechanisms which could potentially cause thesekinds of problems: corrosion, hydrates, a mineral precipitation, sand in producing fluid or mechanical damage. A used wire has a very small diameter so usually it is impossible to exert any significant force to the stuck tools. On the other hand jarring is a very good method to free a tool string, if it is possible. Jarring in a viscous fluid or in highly deviated wells is not very effective.

When long lasting operations do not yield any results, sometimes it is more beneficial to disconnect the wire from the tool string. When such operationsare done, the blowout preventer is closed and aspecial tool called a go-devil is fitted to the wire, then the blowout preventer is opened and the go-devil falls to the rope

socket cutting the wire. Both the go-devil and toolstring have fishing necks, so they could be fished using another slickline tool string or a coiled tubing unit. A coiled tubing could use much greater forces compared to a slickline unit. If a slickline wire would break above the toolstring it would fall into the wellbore and be very difficult to fish it out. Such operations are very costly, and they take a lot of time.

5. Slickline services

Slickline is a type of service where a string of the tools is lowered into a wellbore on a single strand of a solid wire. This wire is typically made from a low carbon steel for a standard service or an alloy for H_2S service. Wire diameters canvary from 1.57 mm (0.062″) to 4.78 mm (0.188″), with the most commonly used in Poland is 2.74 mm (0.108″) diameter wire. On the other hand, a tool string has typically a much larger diameter – about 38 mm (1.5″) and parts of the tool string are screwed together or connected using quick connectors. A typical slickline tool string includes (from top):

- a rope socket – used to securely connect the wire with the tool string,
- stem weight bars (roller stem bars with knuckle joints for deviated wells) – used to exert weight to properly run wire into the wellbore against a well pressure,
- mechanical jars – used to enable upward and downward jarring,
- a slickline tool or gauges – could perform different functions.

The slickline wire diameter is significantly smaller than the diameter of a work string, so a wire is a crucial part of the assembly, its good shape could determine safety of the operations.

With the use of specialized tools, a slickline service could perform various functions:

- checking if there are no obstructions in the production tubing and if it is safe to run another tool using gauge cutters,
- locating the depth of the tubing shoe,
- running downhole pressure and temperature gauges,
- running in PVT samplers, or bailers to obtain fluids and solid samples from the wellbore,
- running and locking downhole pressure and temperature gauges during well testing,
- opening and closing circulation sleeves,
- running and using downhole mechanical perforators to perforate tubing,
- running and locking plugs in landing nipples,
- running and locking downhole chokes in production wells,
- cleaning well from debris using bailers like sand-bailer or hydrostatic bailer,
- cleaning deposits from the inside wall of landing nipples using scratchers,
- mechanical activation of perforators run on drilling string or tubing,
- fishing and other intervention works.

6. Possible aftereffects of accidents

The aftereffects of accidents depend on the scope of the accident. Usually, only time is compromised, resulting in solely economic consequences – another trip, wasted time etc. More serious accidents can result in crew injuries and significant losses to equipment and the environment. The most serious ones could even end in people's death and environmental disaster caused from a blowout. Safety precautions and measures are used to minimize the risk of accidents and to limit their aftereffects.

7. Safety measures

There are many safety measures to minimize the risks, and they apply to both the working crew and equipment use. Firstly, the crew is acquainted with safety manuals and instructed to the correct way of working and how to react indifferent situations. Before starting a job, a safety meeting is conducted where the following issues are discussed: scope of work, safety rules and possible hazards, crew responsibilities, etc. Personal protective equipment suitable for a given situation is used, safety gloves, safety googles and safety glasses, protective shoes, hard hats, gas detectors, etc. When there is possibility of H_2S occurrence, appropriately trained and equipped well mining rescue service oversee and monitor work.

To minimize the risk of fire or explosion, hazardous zones according to ATEX are marked. In these zones a risk of explosion is likely to occur. All the equipment used in these zones is made to minimize the risk of fire and explosion, and it is certified according to ATEX.

Pressure control equipment is controlled visually every time before the start of a job with particular attention to any wear and damages. If necessary,

seals and O-rings are replaced. Every connection is checked if it is screwed securely. Hydraulic fittings are inspected if they work properly, and if they are clear from debris to ensure proper operation of BOP, stuffing box and liquid chamber. Before the start of the job, a pressure test with the test pressure equal or above the expected pressure is conducted. Moreover, all pressure control equipment is pressure tested at regular intervals with manufacturers specification and NDT tests are conducted. From time to time, pressure control assembly is disassembled, inspected and replaceable parts are changed.

During hoisting operations, only certified shackles and slings are used. A crane operator or a derrick man is acquainted with the scope and specifics of the job at the safety meeting, where communication such as hand signals are discussed. When lifting the equipment, crew stay away from hoisted equipment and use the attached string to help with positioning.

8. Concluding remarks

Despite many hazards and risks, operations during drilling and on live wells prove to be both safe and environmentally friendly. Great attention is paid to appropriate preparation – both the crew and equipment. People are trained, a safety meeting is conducted and safety always discussed as a top priority during works. Internal regulation manuals contain a comprehensive approach to further minimize unexpected situations and tips how to react to them. Such serious effort to prevent and minimize risk brings good results where people's safety is crucial. Also, environmental aspects are not omitted, because all leaks and other accidents, even if they don't harm working people, might do so to the environment.

Good condition of the slickline wire and its proper maintenance is crucial, because it limits available parameters and ensures that all operations could be performed safely and in a timely manner.

References

[1] Beyer J., Trannum H.C., Bakke T., Hodson P.V., Collier T.K.: *Environmental effects of the Deepwater Horizon oil spill: A review*. Marine Pollution Bulletin, vol. 110, iss. 1, 2016, pp. 28–51.

[2] Macuda J., Dubiel S.: *Ocena wpływu otwartej erupcji ropy naftowej na środowisko gruntowo-wodne na przykładzie otworu Daszewo-1*. Wiertnictwo, Nafta, Gaz, vol. 27, no. 1–2, 2010, pp. 251–258.

[3] Fabiańczyk E., Ślusarczyk S.: *Sozologiczne aspekty eksploatacji ropy naftowej i gazu ziemnego ze złoża Barnówko-Mostno-Buszewo*. Górnictwo Odkrywkowe, vol. 54, iss. 3–4, 2013, pp. 121–132.

Journal of Geotechnology and Energy | vol. 38 | no. 1 | 2021 | pp. 11–25

Matthew Efe Takerhi

ORCID: 0000-0002-9098-1177
AGH University of Science and Technology in Krakow

SEPARATION OF NATURAL GAS LIQUIDS AND WATER FROM GAS CONDENSATE

Date of submission:
21.05.2021

Date of acceptance:
14.07.2021

Date of publication:
31.07.2021

https://journals.agh.edu.pl/jge

Abstract: Unlike dry gas reservoirs, condensate gas reservoirs contain a considerable amount of natural gas liquids which should be extracted to maximize energy usage. This paper uses Bryan ProMax to set up the processing units for the recovery of natural gas liquids and removal of water. The parameters for the simulation were a gas composition which assumes a sweet gas content. The outcome of the simulation includes reduction of water content below 7 lbm/MMscf, recovery of methane and recovery of propane and isobutane only. The glycol dehydration unit minimized water impurity, while cooling with Joule–Thomson valve and heat exchangers help in methane recovery and separation from natural gas liquids. The results show that natural gas liquid recovery which depends on gas composition can be recovered by controlling the conditions of several units, namely heat exchangers, flash vessels, cold separators, fractionators, stabilizers with their reboilers and condensers.

Keywords: gas condensate, Natural Gas Liquids (NGL), fractionations

1. Introduction

In 1910, a displeased motorist complained to Dr Walter Snelling of the U.S Bureau of Mines that half of his gas tank had disappeared when he got home. Snelling examined a sample and discovered that the disappearing liquid was evaporating gases. He made his distillation column using an old water heater, some copper tubing, and wire-wrapped glass bottles. This allowed him to collect the gases as liquid and to patent the first process for capturing natural gas liquids. By so doing Snelling was able to separate the fraction of disappearing liquid into a separate product using fractional distillation [1]. In the middle of the 20th century, the natural gas business was not clearly noticed, it was an obscure business in production and exploration companies. The growth in the petrochemical and transportation industry led to more demand for natural gas liquids. More recently, the increasing supply of natural gas liquids has put the product on the business agenda [1].

Natural gas liquids (NGL) are produced from natural gas wells or from associated gas oil wells. In gas wells, natural gas liquids also called condensate which is separated at the separator and further removal is carried out in the gas plant. Gas plants clean up contaminates in the gas and NGL, separates NGL from the natural gas, and then several fractionators separate the NGL from each other. The various NGL, each meeting its own specification, move into several shared markets such as refining and petrochemical feedstocks, burner tips and internal combustion engine [1].

Natural gas mainly contains methane and natural gas liquids, which include ethane, LPG (propane and butane), gas-condensate. Methane is commonly known as fuel gas used for heating and power plants. Additionally, NGL are also valuable as separate products.

Ethane is very valuable in the petrochemical industry but as the most volatile NGL it is used almost exclusively as a petrochemical feedstock; in the petrochemical plants, ethane is converted to ethylene, and changed to polyethylene or ethyl alcohol, or various ethylene-based petrochemicals.

Propane is too volatile to be placed in gasoline and too valuable and heavy to be left with natural gas, it is used as a fuel for heating, cooking and sometimes lighting; as a petrochemical feedstock to make both ethylene and propylene as co-products; as a motor fuel; petrochemical companies use propylene to make polypropylene and isopropyl alcohol and other products.

Butane is less volatile than propane but is still shipped and handled under pressure as liquids. Normal butane is used in the fuel market for heating and cooking, though not as much as propane. It is used as a gasoline-blending component to add little volatility. It is also used in the petrochemical plants to produce ethylene, propylene, butylene and butadiene, while LPG are used for cooking and heating.

Natural gasoline exist as a liquid at room temperature and pressure, has a low octane number, although refineries can clean up natural gasoline and even upgrade it and blend it with better components to make it suitable for sale at gas stations. Natural gasoline is also used as diluents for very heavy crude oils, and it reduces the viscosity of crude oils so it can be moved in a pipeline [1]. It is therefore profitable to separate the ethane, propane and butane and gasoline from the natural gas.

1.1. Description of NGL extraction

The NGL are first extracted from the natural gas and later separated into different components. Let us focus on optimization of the gas-condensate exploitation processes in the recovery of LPG and ethane [1]. The order of processes in natural gas processing depends on its composition. The first process is separation, which consists of one or more separators used to set condensation and remove the free water, two-phase gas liquid separators are used for separation of two-phase gas liquids, while three-phase separators are used for three-phase component containing oil, gas, and water.

The well stream from the gas condensate reservoir undergoes staged separation to separate the gas from the condensate. Stage separation is the process by which gaseous and liquid hydrocarbons are flashed into vapor and liquid phases by two or more separators. The aim of separation is to achieve maximum liquid recovery and stabilization of the gas products [2]. A large pressure reduction in a single separator will cause flash vaporization and is a safety hazard. In the first stage of separation, water content is usually reduced to 5%; there must be a minimum pressure difference between each stage of the separation to ensure satisfactory performance in pressure and level control loops.

As gas flows into the separator, the inlet diverter causes a sudden change in momentum which results in settling of the liquids droplets, other liquids droplets fall to the bottom of the separator due to gravity and are separated into oil and water phase. Vapor rises upwards and passes through the demister, which have tiny perforations that condense the tiny vapor in the gas into the liquids, which fall back to the bottom of the separator. The second separator is also known as the intermediate separator, its pressure is reduced for optimum recovery of methane gas and natural gas liquids, usually to the level of atmospheric pressure where temperature should be below 100°C, and water content will be reduced to about 2%. The pressure of this separator should be modified to ensure that the optimum amount

of natural gas liquids is recovered from the gas stream. The condensate stream is flashed into the low-pressure separator. Processing facilities would often have either two or three stage separators. In two stage separators, only one intermediate separator is possible while a three-stage separator allows for either one operating at second or third stage suction pressure [3].

The last separator is usually at standard conditions of 15°C and 14.7 psi. The gases from the last stage separator have lost so much pressure that they must be recompressed for transportation [2: 43] and should be cooled and recompressed before transfer to the natural gas pipeline. Natural gas liquids from the bottom of the separator are dehydrated. Table 1 shows stage separation guidelines [3: 45]. The condensates are sent to the refinery while raw natural gas is transported to a gas processing plant. The natural gas is treated to remove acid gases. For fractionation of the natural gas liquids, Abdel Aal et al., suggests two essential requirements for designing a fractionating unit: understanding the process used for separation; the guidelines to determine the sequence of separation [4].

Table 1. Stage separation guidelines [3]

Initial separation pressure		
[psig]	[kPa]	number of stages
25–125	170–860	1
125–300	860–2100	1–2
300–500	2100–3400	2
500–700	3400–4800	2–3

1.2. Gas dehydration process

The next unit is the dehydration unit which uses either regenerable absorption or a regenerable adsorption unit for removing water vapor from gas. In an absorption process, a special solvent is used as the absorbent, which selectively absorbs water vapor from the rising gas vapor, as it moves down the column. Well known absorbents used include glycols, among which triethylene glycol (TEG) is most used and which works with gas temperatures as high as 120°C. The other glycols include ethylene glycol (EG), diethylene glycol (DEG), tetraethylene glycol (TREG) and propylene. For the adsorption process, activated charcoal or molecular sieves are used as the adsorbent [4: 44–50]. Table 2 contains the operational parameters of a glycol dehydration unit [5: 142], Table 3 presented the fractionator operating conditions.

Removal of water from gas helps to prevent hydrate formation when temperature drops in transmission and distribution system and prevents corrosion problems because of the condensation of water vapor due to high pressure drops or cold temperatures.

Table 2. Operational parameters of a glycol dehydration unit [5: 234]

Parameters	Values
Pressure in inlet separator and glycol contactor	Feed gas pressure
Feed gas pressure	600–1200 psia
Lean glycol temperature	10°F hotter than the inlet gas temperature
Reboiler temperature	375°F to 390°F
Minimum glycol circulation rate	2 gallons of glycol per one pound of water
The regenerator, typical reboiler temperature	350°F (176.6°C)

Table 3. Typical fractionator operating conditions [4]

Fractionating column	Operating pressure [psig]	Number of trays	Tray efficiency
Deethanizer	375–450	25–35	60–80
Depropanizer	240–270	30–40	80–90
Debutanizer	70–100	25–35	85–95
Butane Splitter	80–100	60–80	90–100

2. Research problem and the method of solution

The data for the natural gas condensate well stream which is used for the simulation is shown in Table 4 which contains some water and hydrocarbons from methane to decane at 100°F, 970 psia with a standard volumetric flow of 290 MMscf. The challenge is to recover the hydrocarbons and meet the product specifications. For the natural gas product (fuel gas), some specification require at least 70% mole of methane with a maximum water content not exceeding 7 lbm/MMscf, and its dewpoint temperature should be sufficiently low. This is to ensure that at any temperature during operations, liquids are not formed because this may cause hydrates or corrosion. The problem also concerns fractionation of natural gas liquids (C2 to C10+) to obtain ethane, propane, and butane.

In the simulation used for obtaining the result, the sequence of operation is in the following order: dehydration of natural gas stream, demethanizer operation and fractionation of natural gas liquids. Bryan ProMax is used to estimate the content of water in the input stream from the well, and that of the output stream from the glycol contactor, in other to determine if dehydration has been fulfilled sufficiently.

From the literature review, the operating parameters for the separator, glycol dehydration units, and

the fractionators were summarized in Tables 1–3, and can be used as a reference for simulation. Then a review is carried out to find the optimal technologies to separate those valuable components – methane, ethane, LPG, gas-condensate. Finally, the methodology for processing this well is suggested as follows: at first, water is removed from the stream by dehydration unit using triethylene glycol; then, methane is recovered as a fuel gas stream, propane and butanes are recovered and finally the remaining heavier hydrocarbons, C5+ (hydrocarbons). To achieve the optimal conditions for these gas processes, a simulation of a gas plant was created using ProMax version 4.0 software with some facilities like: propane refrigeration loop, the Joule–Thompson valve, the turbo expander included.

3. Results

The gas plant has been simulated by 3 main parts: dehydration unit, demethanizer processing unit and fractionation of natural gas liquid which was restricted to only the depolarizer column. The various processing units represented in Brayan Pro-Max are dehydration unit, demethanizer unit and depropanizer units respectively as shown in Figures 1, 4, and 7.

3.1. Operation of the dehydration unit

The dehydration unit is shown in Figure 1, where the input stream contains hydrocarbon components from methane to decane as shown in Table 4, Figure 2 and 3, at 100°F of and 950 psia, with standard vapor volumetric flow of 153.5 MMscfd and standard liquid volumetric flow of 2799.78 sgpm as shown in Figure 2. Analysis of the streams with the glycol contactor indicate water content of 55.37 lbm/MMscf at the input stream (wet gas feed), and 6.96 lbm/MMscf at the output stream (stream 4), with the triethylene glycol flow of 43.07 sgpm (std liquid volumetric flow), as shown in Figure 2. Water dew temperature is 100.02°F at the input stream (wet gas stream) and 35.91°F at the output stream, where water dew point temperature represents the temperature where water begins to form. To meet the specification of water which is below 7 lbm/MMscf, the specifier of the standard liquid volumetric flow of triethylene glycol was adjusted from water-fed multi-plied by 3 to water-fed multiplied by 5.9 which resulted in meeting the water content value at the output stream as shown in Figure 2.

The dehydration process is such that triethylene glycol was pumped at a rate of the water-fed multiplied by a constant value, which resulted in triethylene glycol flow of 43.07 sgpm of glycol in the glycol maker shown in Figure 2. The triethylene glycol produced in the triethylene glycol makeup unit is transported by the glycol pump which increases the temperature of the flowing stream, which is subsequently cooled by the gas/glycol exchanger. Next the stream is passed through a recycle block to the glycol contactor, a recycle block is a unit where the initial guesses are specified – they include: temperature, pressure, composition (100% triethylene glycol) and molar flow [lbmol/hr]. Those parameters are shown in Figure 3. The temperature of triethylene glycol should be below 110 to prevent loss in the glycol contactor. Initially, triethylene glycol is passed into the top of the contactor resulting in downward flow to the bottom of the contactor simultaneously absorbing water from the rising natural gas stream on contact.

Table 4. Gas composition used for the simulation

Component	Mole percent [% mole]	Mole fraction [Yi]
N_2	23.83599	0.23836
CH_4	54.32819	0.543282
C_2H_6	5.079988	0.0508
C_3H_8	2.678428	0.026784
i-C4	0.424063	0.004241
n-C4	0.764013	0.00764
i-C5	0.233935	0.002339
n-C5	0.176109	0.001761
n-C6pent	0.118333	0.001183
2-methylpentane	0.174827	0.001748
3-methylpentane	0.963353	0.009634
n-C7	0.462133	0.004621
2-methylhexane	0.250883	0.002509
C8	0.352549	0.003525
2-methylheptane	0.500026	0.005
3-methylheptane	0.688129	0.006881
C9	0.530791	0.005308
2-methyloctane	0.544235	0.005442
3-methyloctane	0.401946	0.004019
C10	0.328732	0.003287
2-methylnonane	0.332425	0.003324
3-methylnonane	0.307783	0.003078
C10+	6.523137	0.065231
H_2O	0.07636	0.0007636

Subsequently after flowing out of the glycol contactor, rich triethylene glycol passes through a reflux coil and Joule–Thompson valve, the reflux coil helps to add some heat, and the Joule–Thompson valve reduces the pressure of the stream by 890 psia which also reduces the temperature by 8.78°F, and subsequently passed to the rich flash separator to produce a flash gas, and

a condensate liquid which is a mixture of triethylene glycol and water. The triethylene glycol and water mixture are passed into the glycol regenerator for recovery, where mostly triethylene glycol is produced from the bottom stream and water from the top stream. The stream from the top of the glycol regenerator is passed into the condenser for more recovery of triethylene glycol. From the condenser, water vapour is recovered and heat is transferred from the condenser to an exchanger used to warm the glycol contactor end products with the QRecycle block. The QRecycle block is used to provide initial estimates of recycled energy.

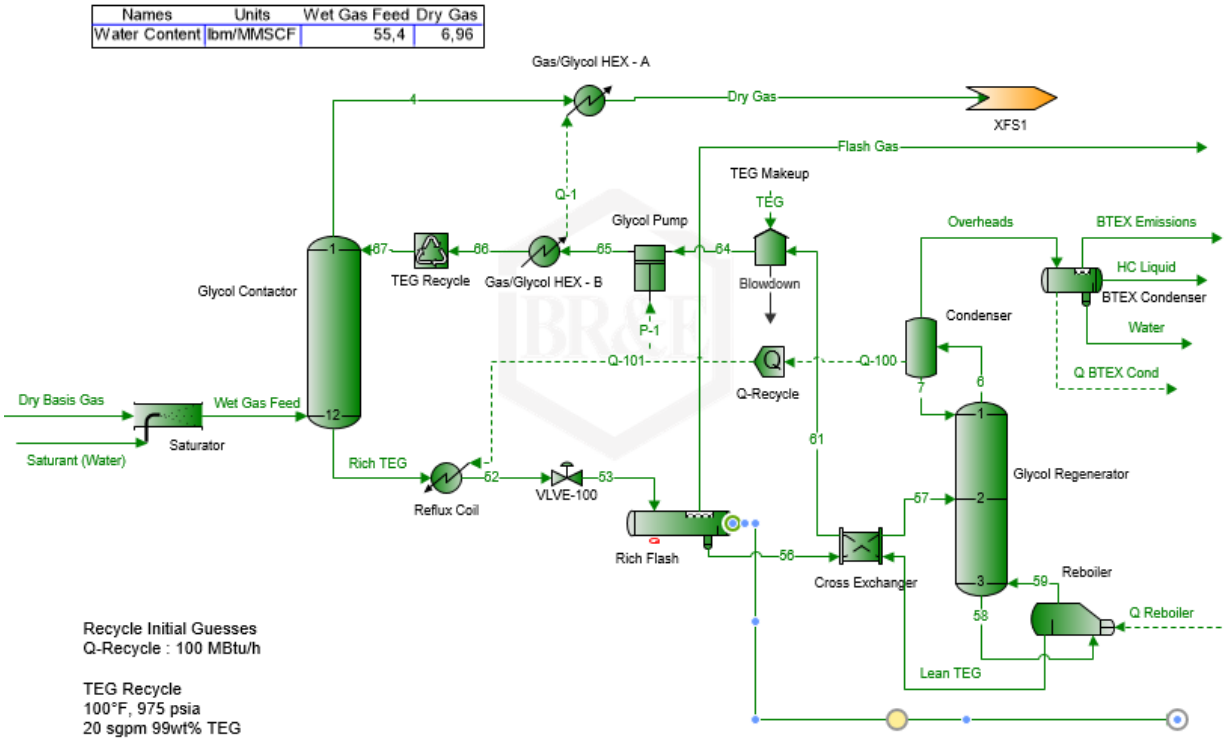

Fig. 1. Dehydration unit for water removal

3.2. Conditions for running dehydration

The conditions for running the glycol dehydration are summarized in Table 5. It shows that the glycol contactor inlet stream with 12 stages and a pressure of 970 psia which drives the pressure of the glycol contactor. Since there is no reboiler for the glycol contactor, the temperature and the pressure are driven by the property of the input stream (wet gas feed), which is the only input to the glycol contactor. The gas/glycol HEX-A and JT valve (vlve-100) are used to cool the stream with a temperature drop of 89.43°F and 8.82°F respectively. The Reflux Coil was used to add heat to the stream with a temperature increase of 12.81°F, while the glycol pump operation result pressure drop of 965.3 psia, indicating high flow and temperature increases of 1.79°F. Across the glycol regenerator there was small pressure drop and heat was added by the reboiler resulting in an increase in temperature of 86°F to remove the water content, while the condenser aids in the recovery of triethylene glycol.

3.3. Demethanizer processing unit

The conditions of the dehydrated stream (inlet stream) are 955 psia, 113°F and at 153.66 mmscfd (standard vapor volumetric flow) as shown in Figure 5, with 63% mole of methane with other hydrocarbon components. There are two output streams: the first output stream product is fuel gas, predominantly methane, with about 63.5% mole of methane at 293 psia and 83°F with 153.5 mmscfd (standard vapor volumetric flow); the other output product stream is a liquid stream – unlike the first output product, it contains almost no methane of about 5.525e-06% mole and also serves as the input to the fractionation processing unit, the preceding values are shown in Figure 6.

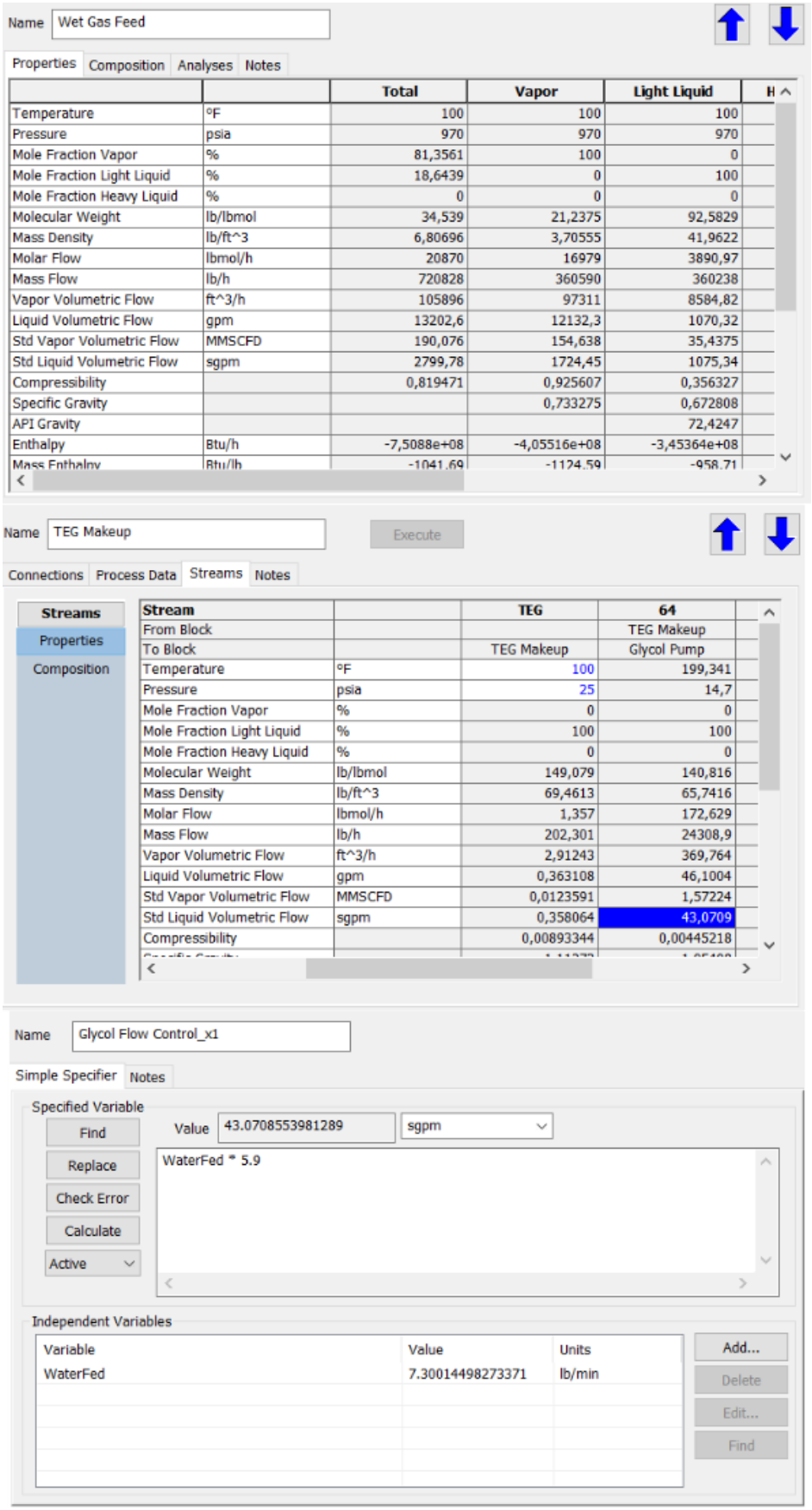

Fig. 2. Conditions of the inlet stream to the glycol contactor with conditions at the triethylene glycol and its specifier

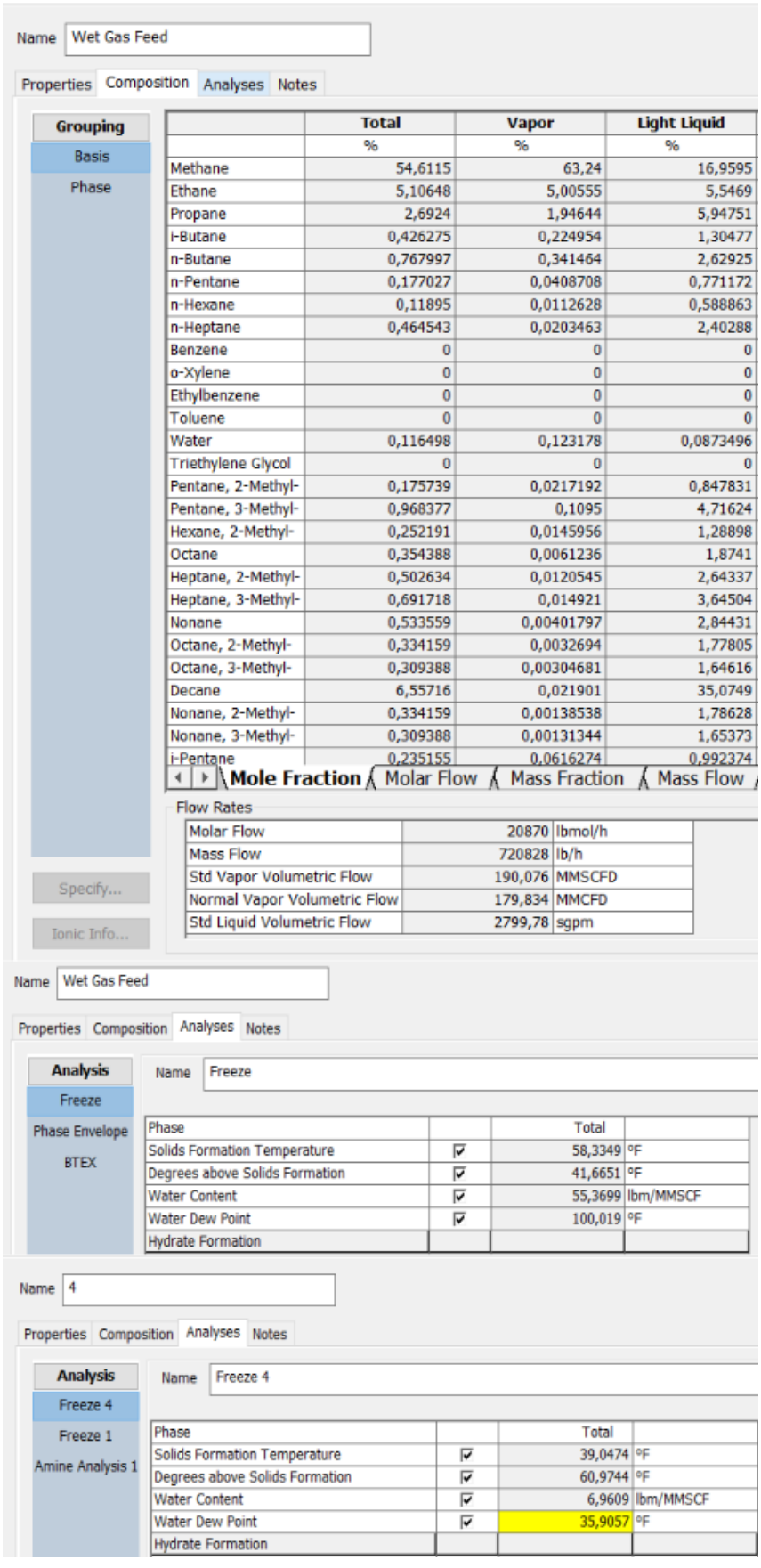

	Total	Vapor	Light Liquid
	%	%	%
Methane	54,6115	63,24	16,9595
Ethane	5,10648	5,00555	5,5469
Propane	2,6924	1,94644	5,94751
i-Butane	0,426275	0,224954	1,30477
n-Butane	0,767997	0,341464	2,62925
n-Pentane	0,177027	0,0408708	0,771172
n-Hexane	0,11895	0,0112628	0,588863
n-Heptane	0,464543	0,0203463	2,40288
Benzene	0	0	0
o-Xylene	0	0	0
Ethylbenzene	0	0	0
Toluene	0	0	0
Water	0,116498	0,123178	0,0873496
Triethylene Glycol	0	0	0
Pentane, 2-Methyl-	0,175739	0,0217192	0,847831
Pentane, 3-Methyl-	0,968377	0,1095	4,71624
Hexane, 2-Methyl-	0,252191	0,0145956	1,28898
Octane	0,354388	0,0061236	1,8741
Heptane, 2-Methyl-	0,502634	0,0120545	2,64337
Heptane, 3-Methyl-	0,691718	0,014921	3,64504
Nonane	0,533559	0,00401797	2,84431
Octane, 2-Methyl-	0,334159	0,0032694	1,77805
Octane, 3-Methyl-	0,309388	0,00304681	1,64616
Decane	6,55716	0,021901	35,0749
Nonane, 2-Methyl-	0,334159	0,00138538	1,78628
Nonane, 3-Methyl-	0,309388	0,00131344	1,65373
i-Pentane	0,235155	0,0616274	0,992374

Fig. 3. Input stream to the dehydration unit

Table 5. The conditions for running dehydration part

Units	Inlet pressure [psia]	Pressure drop [psia]	Inlet temperature [°F]	Temperature change [°F]	Other properties
Glycol contactor	970	10	92.7–91.4	6.7	12 stages
Gas/glycol HEX-A	980	5	199.87	89.43	Heat duty: –1.8e+06 btu/h
Reflux coil	970	5	79.09	–12.81	Heat duty: –563,106 kJ/h
Glycol pump	14.7	965.3	199.34°F	–1.79	Power: 52.33 hp Overall efficiency: 68%
JT valve: VLVE-100	965	890	103.23	8.78	–
Rich flash	75	0	94.41	0	–
Glycol regenerator	70	0.5	98.86	192.69	Reflux ratio target: 1 Reflux ratio value: 0.1 Boilup ratio target: 0.2289 Boilup ratio value: 0.1969 Reboiler temperature target: 400°F Reboiler temperature value: 400°F
Condenser for glycol	14.7	0	218.90	11.58	Heat duty: –64869.8 btu/h
Glycol regenerator reboiler	15.2	0	314.50	–86	Heat duty: 286e+06 btu/h
Cross exchanger	–	–	–	–	Pressure drops across lean TEG to blowdown: 0.5 psia. And temperature drops by 201.07°F Pressure drop across rich flash and stream to inlet to glycol regenerator: 5 psia. And temperature increased by –205.88°F

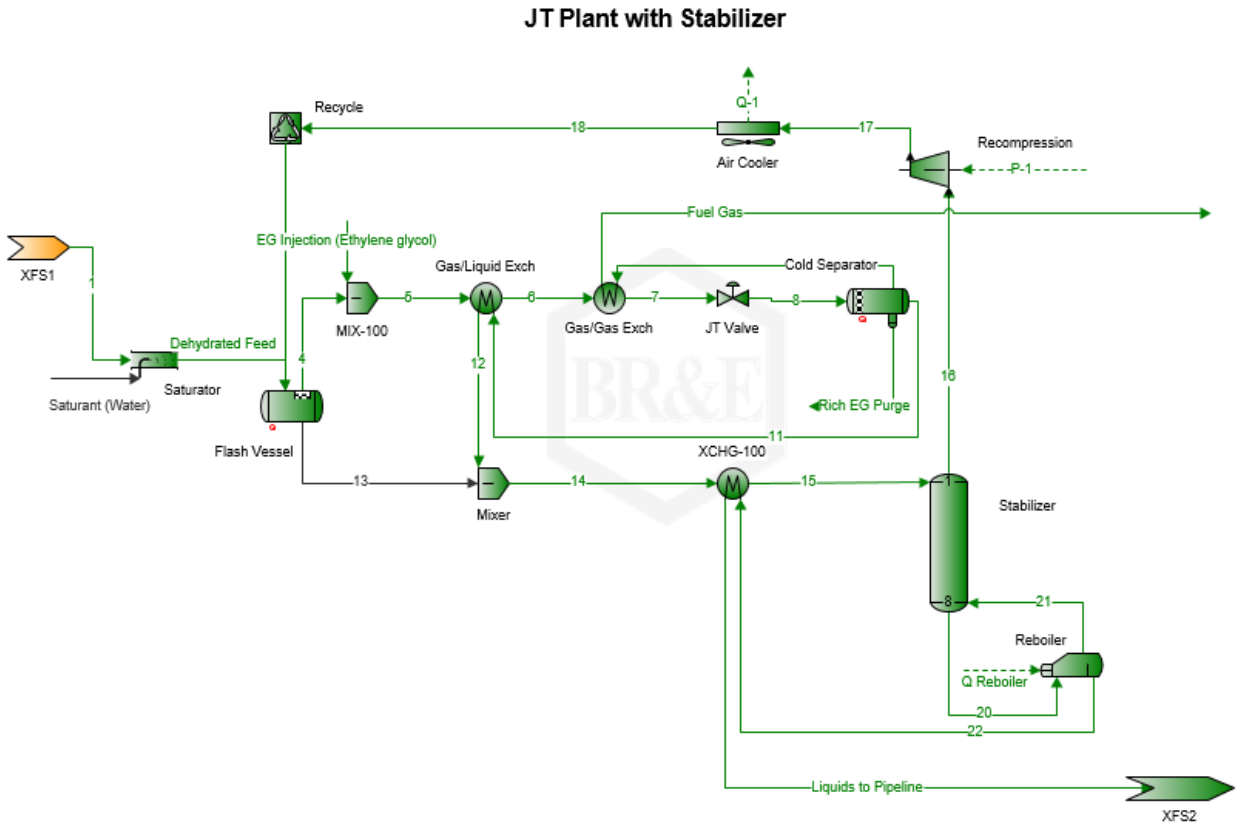

Fig. 4. Methane and nitrogen removal units to separate methane and nitrogen as sales gas

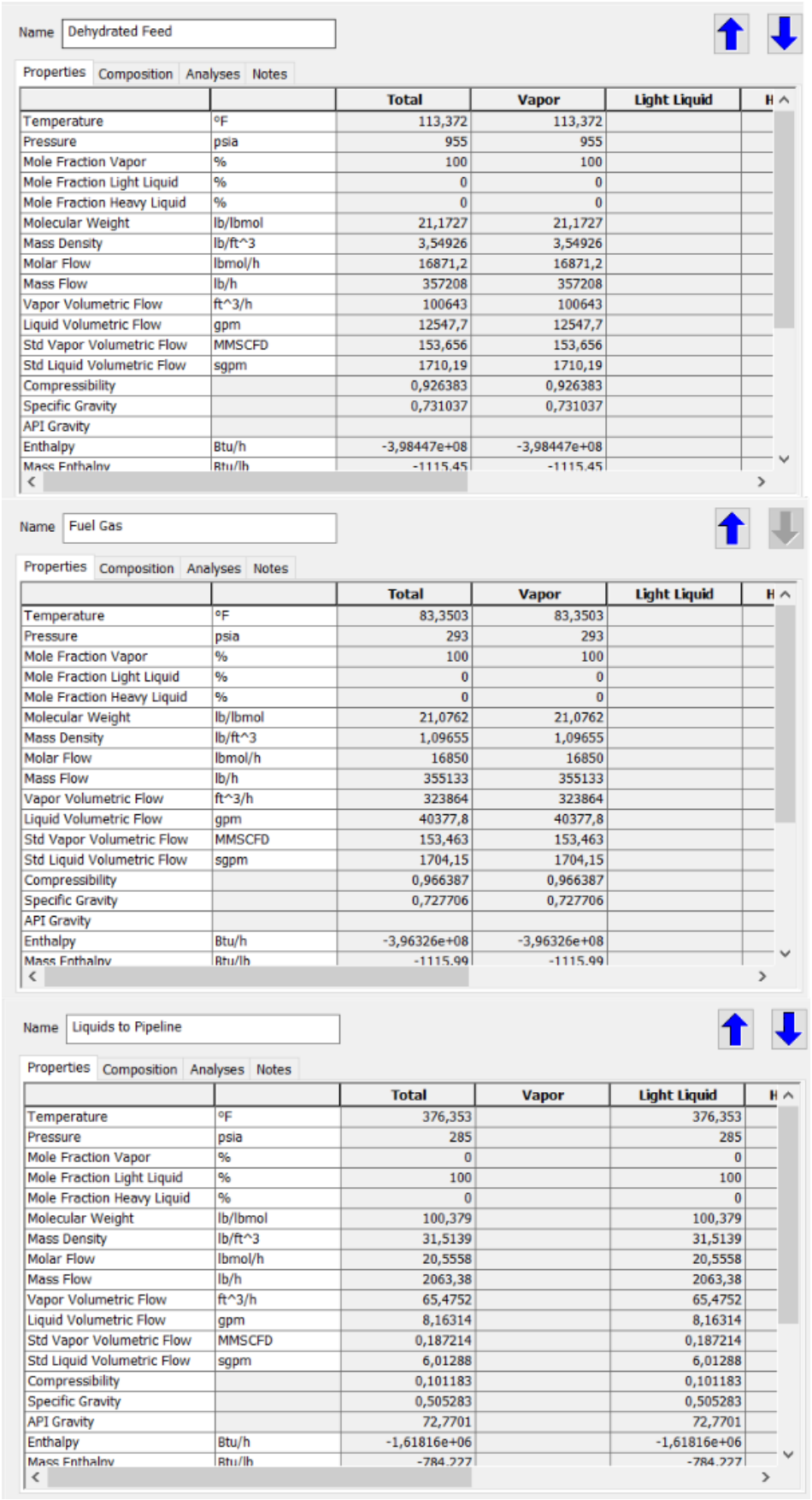

Name: Dehydrated Feed

Properties | Composition | Analyses | Notes

		Total	Vapor	Light Liquid
Temperature	°F	113,372	113,372	
Pressure	psia	955	955	
Mole Fraction Vapor	%	100	100	
Mole Fraction Light Liquid	%	0	0	
Mole Fraction Heavy Liquid	%	0	0	
Molecular Weight	lb/lbmol	21,1727	21,1727	
Mass Density	lb/ft^3	3,54926	3,54926	
Molar Flow	lbmol/h	16871,2	16871,2	
Mass Flow	lb/h	357208	357208	
Vapor Volumetric Flow	ft^3/h	100643	100643	
Liquid Volumetric Flow	gpm	12547,7	12547,7	
Std Vapor Volumetric Flow	MMSCFD	153,656	153,656	
Std Liquid Volumetric Flow	sgpm	1710,19	1710,19	
Compressibility		0,926383	0,926383	
Specific Gravity		0,731037	0,731037	
API Gravity				
Enthalpy	Btu/h	-3,98447e+08	-3,98447e+08	
Mass Enthalpy	Btu/lb	-1115,45	-1115,45	

Name: Fuel Gas

Properties | Composition | Analyses | Notes

		Total	Vapor	Light Liquid
Temperature	°F	83,3503	83,3503	
Pressure	psia	293	293	
Mole Fraction Vapor	%	100	100	
Mole Fraction Light Liquid	%	0	0	
Mole Fraction Heavy Liquid	%	0	0	
Molecular Weight	lb/lbmol	21,0762	21,0762	
Mass Density	lb/ft^3	1,09655	1,09655	
Molar Flow	lbmol/h	16850	16850	
Mass Flow	lb/h	355133	355133	
Vapor Volumetric Flow	ft^3/h	323864	323864	
Liquid Volumetric Flow	gpm	40377,8	40377,8	
Std Vapor Volumetric Flow	MMSCFD	153,463	153,463	
Std Liquid Volumetric Flow	sgpm	1704,15	1704,15	
Compressibility		0,966387	0,966387	
Specific Gravity		0,727706	0,727706	
API Gravity				
Enthalpy	Btu/h	-3,96326e+08	-3,96326e+08	
Mass Enthalpy	Btu/lb	-1115,99	-1115,99	

Name: Liquids to Pipeline

Properties | Composition | Analyses | Notes

		Total	Vapor	Light Liquid
Temperature	°F	376,353		376,353
Pressure	psia	285		285
Mole Fraction Vapor	%	0		0
Mole Fraction Light Liquid	%	100		100
Mole Fraction Heavy Liquid	%	0		0
Molecular Weight	lb/lbmol	100,379		100,379
Mass Density	lb/ft^3	31,5139		31,5139
Molar Flow	lbmol/h	20,5558		20,5558
Mass Flow	lb/h	2063,38		2063,38
Vapor Volumetric Flow	ft^3/h	65,4752		65,4752
Liquid Volumetric Flow	gpm	8,16314		8,16314
Std Vapor Volumetric Flow	MMSCFD	0,187214		0,187214
Std Liquid Volumetric Flow	sgpm	6,01288		6,01288
Compressibility		0,101183		0,101183
Specific Gravity		0,505283		0,505283
API Gravity		72,7701		72,7701
Enthalpy	Btu/h	-1,61816e+06		-1,61816e+06
Mass Enthalpy	Btu/lb	-784,227		-784,227

Fig. 5. Conditions at the inlet stream to the flash vessel (dehydrated stream), fuel gas and natural gas liquid gas

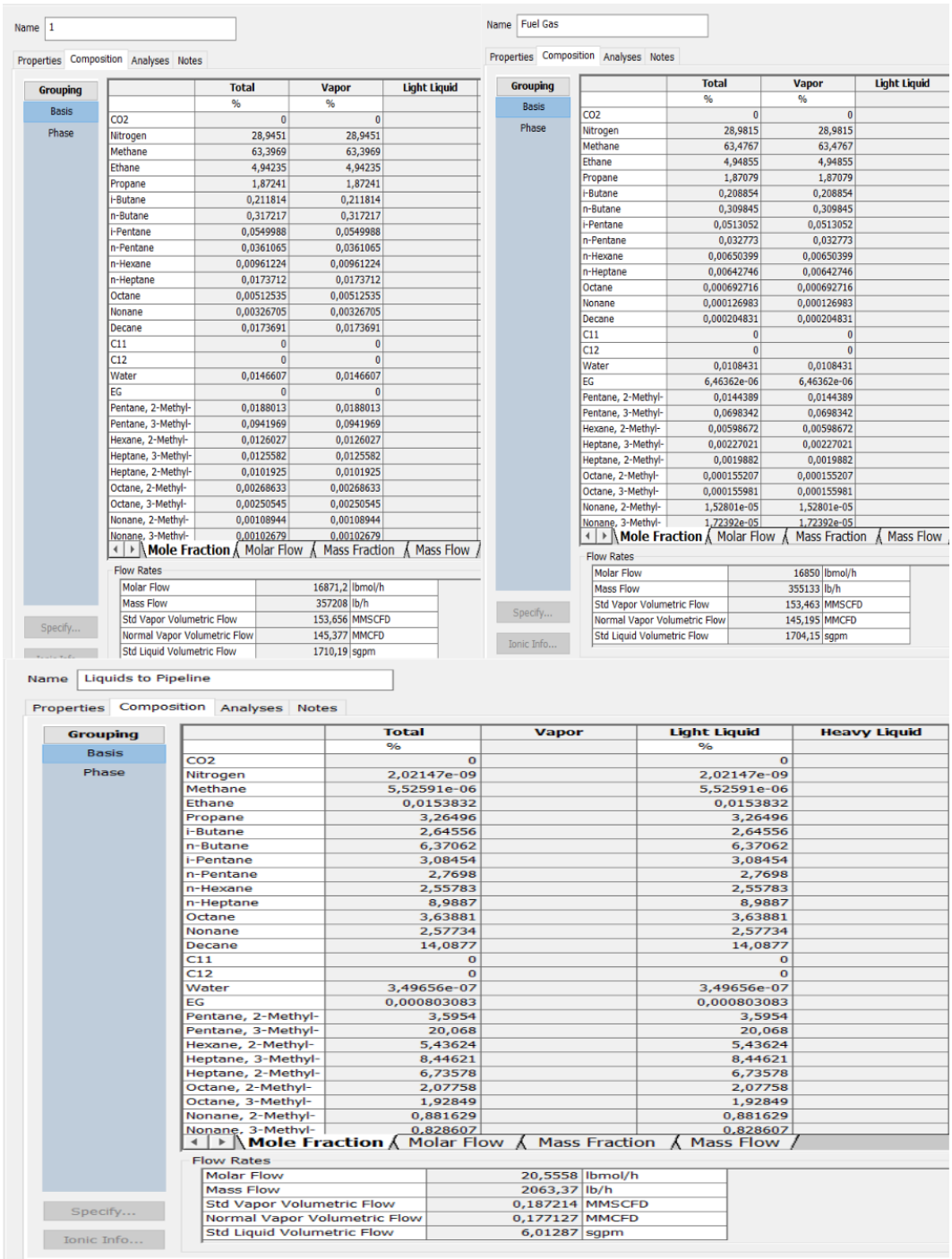

Fig. 6. Data of two outlet streams from the demethanizer and output stream for fuel gas and natural gas liquid

3.4. Conditions for running demethanizer operations

The conditions for running the demethanizer operation is summarized in Table 6, where the flow from the input stream which have been dehydrated is saturated with water before being sent with compressed vapor from the recycle stream into the flash vessel, where a pressure drop of 20 psia occurs across the flash vessel. From the flash vessels the light components are mixed with ethylene glycol and cooled by the gas/liquid and gas/gas exchangers, and subsequently by the Joule–Thompson valve before it is sent to the cold separator. The gas/gas exchanger contributes the greatest drop in temperature, cooling by 59.6°F, followed by the Joule–Thompson valve with 34.9°F and gas/liquid exchanger with 0.5°F.

Table 6. The conditions for running demethanizer operations

Units	Inlet temperature [°F]	Temperature change [°F]	Inlet pressure [psia]	Pressure drop [psia]	Other properties
Flash vessel	Dehydrated feed: 110.27 Recycle feed: 120	temperature change = 2.5°F	Dehydrated feed: 955 Recycle feed: 900	22	–
MIX-100	107.9	0	898	0	–
Gas/liquid exchanger	107.8	0.6 (cooling)	898	5	Heat duty: 60,592.99 btu/h
Gas/gas exchanger	Stream 6: 107.2 Stream 9: 14.94	Stream 6: 59.6°F (cooling) Stream 9: –68.4 (heating)	Stream 6: 893 Stream 9: 298	Stream 6: 5 Stream 9: 5	Heat duty: 1.016e+07 btu/h
JT valve	50	34.9°F (cooling)	888	588	Joule–Thomson coefficient: 0.06095°F/psi
Mixer	Stream 12: 60	0	Stream 12: 293	0	–
XCHG-100 liquid exchanger	Stream 56: 94 Lean TEG: 400	Stream 56: –206 (heating) Lean TEG: 201.07 (cooling)	Stream 56: 75 Lean TEG: 15.2	Stream 56: 5 Lean TEG: 0.5	–85121.997 Btu/h
Cold separator	14.2	0.15	300	2	–
Air cooler	289.7	169.7	905	5	–
Recompression	158.38	–129.25 (heating)	288	–617 (increased pressure)	Performance curve type: isentropic (adiabatic) efficiency: 85%
Stabilizer	120	Inlet: –38.38 262.84° across all stages	290	2	Number of stages: 8
Stabilizer reboiler	357.21	–62.14 (heating)	290	0	–

Cold separator with a pressure drop of 2 psi and temperature drop on 0.15°F, aids the separation of gas from the natural gas liquids. Natural gas from the cold separator cools the incoming stream to the gas/gas exchanger, simultaneously warming itself, before being sent out as the natural gas product containing mainly methane. Natural gas liquids from the cool separator are used as coolant for the gas/liquid exchanger, before moving to the mixer, then to the XCHG-100 (vapor/liquid exchanger), where heating by the liquid stream from the stabilizer reboiler takes place. This causes a temperature rise of 60°F in the stream to XCHG-100 exchanger. The stabilizer unit recovers more light components through its stages in addition, through heating the bottom components in its reboiler. Across the stablizer, from its input to the top, where the lighter components passes out, temperature increases by 38.38°F while temperature change along all its stages of the stabilizer is about 262.84°F with a pressure drop of 2 psi and the reboiler provides heat with temperature increase of 63.39°F.

The product of the reboiler includes natural gas liquids and vapor. The natural liquids are sent to cool the input of the stabilizer in the XCHG-100 (vapor/liquid exchanger) before it is sent as an input to the fractionation unit to obtain various natural gas liquid products. The vapor stream produced from the stabilizer is sent for recompression which increases pressure by 617 psia resulting in a temperature rise of 129°F. Next, the pressurized stream is sent to the air cooler which reduces the temperature by 169°F, which appears to compensate for the drastic increase in temperature due to recompression. The cooled vapor from the air cooler becomes the recycle value which is sent to the flash vessel.

3.5. Depropanizer processing unit

The liquid stream from the demethaizer unit serves as the input to the fractionation unit (Fig. 7). The simulation was not feasible for the deethanizer unit. The input stream was removed from the deethanizer column and connected to the depropanizer column which resulted in a feasible simulation and with a propane product containing 14.62% mole i-butane and 30.40% mole n-butane while product of the bottom stream contained 0.37% mole i-butane and 1.8% mole n-butane as shown in Figure 8. The simulation was infeasible to separate i-butane from n-butane and other heavier hydrocarbons accounted for the rest of the mole percent.

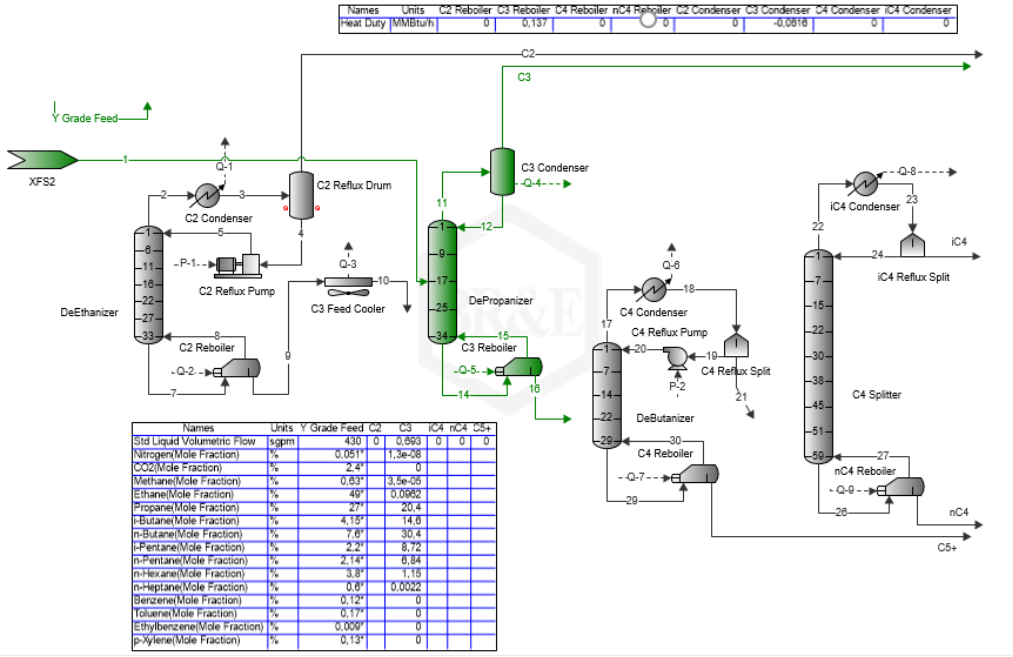

Fig. 7. Fractionation to separate C5+, i-C4, n-C4, C3, C2 components

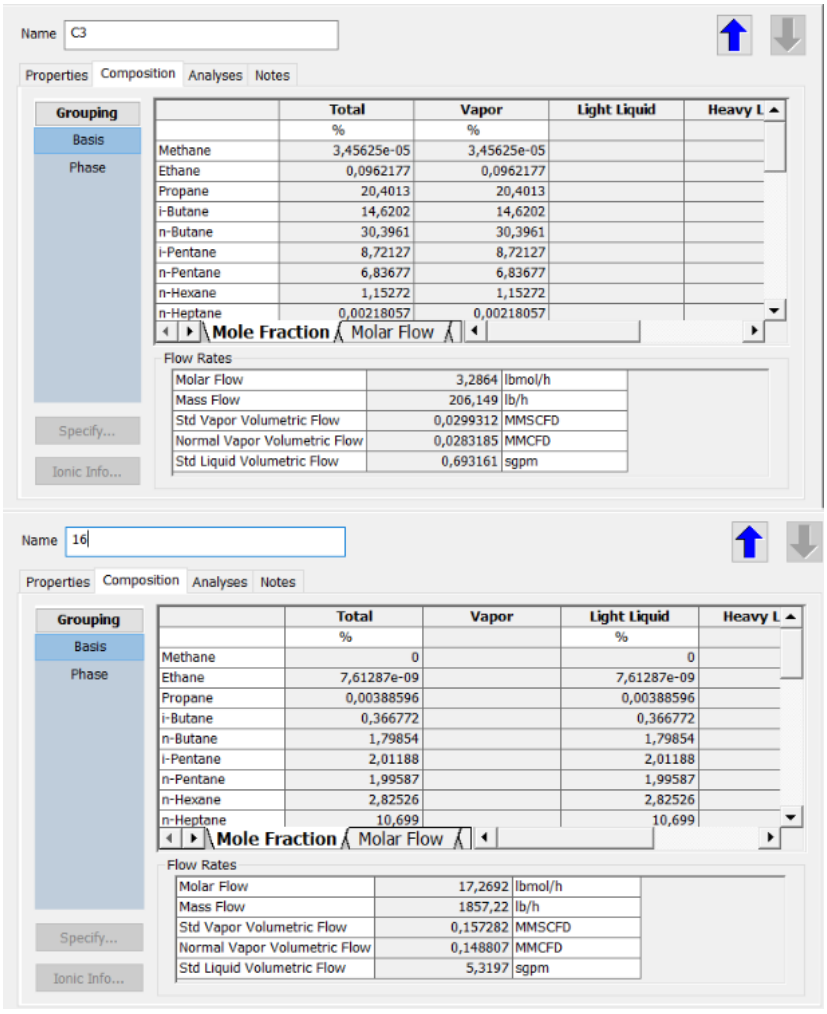

Fig. 8. Propane products from the depropanizer in stream C3 and the heavier hydrocarbon products in stream 16

3.6. Conditions for running fractionation

The natural gas liquid stream from the demethanizer was first sent to the deethanizer column, but results in an infeasible solution, and was repeated for other columns. The only feasible solution was passing natural liquid to the depropanizer column which was isolated from the debutanizer column where input stream conditions were 376.54°F, 285 psia and 0.1872 MMscfd (standard vapor volumetric flow), and 6.31 MMscfd (standard liquid volumetric flow) as shown in Figure 8. The operation is summarized in Table 7 with 34 stages, and as shown in Figure 9, the specification target includes 99.9% recovery rate for propane while the actual value in the simulation is 99.9001% and the bottom product specification target of isobutane was 98% while the actual value was 11.64%. The reflux ratio target value is 2, as well as the value used.

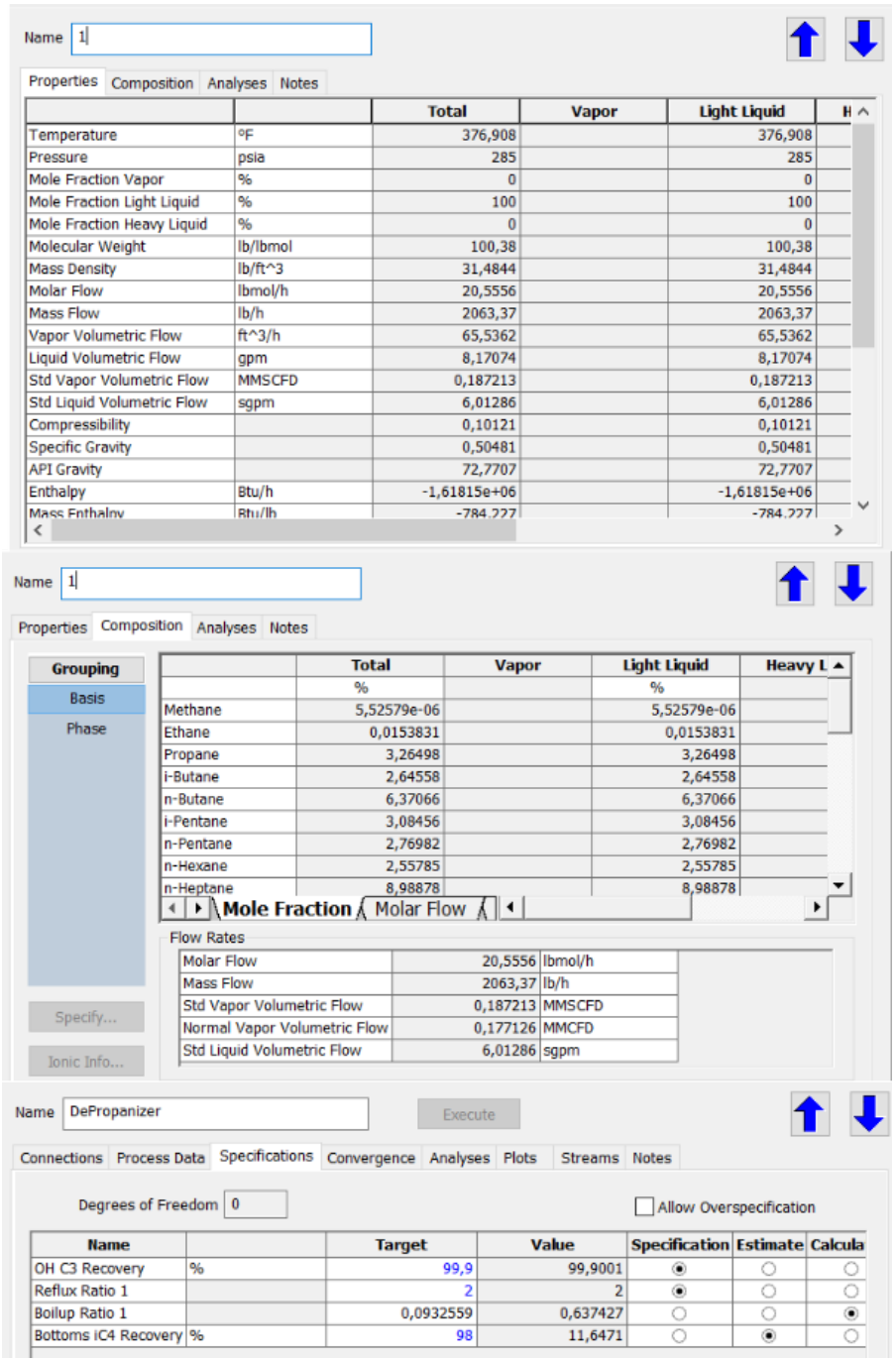

Fig. 9. Conditions of the inlet stream to the depropanizer with its composition and the specification of the depropanizer

Table 7. The conditions for running fractionation

Units	Inlet temperature [°F]	Temperature change [°F]	Inlet pressure [psia]	Pressure [psia]	Other properties
Depropanizer	376.54	Temperature drop across all stages: 178.6	285	Pressure drop across all stages: 2	Number of stages: 34 OH C3 recovery: 99.9% Reflux ratio target and value: 2 Boilup ratio target: 0.0932559 Boilup ratio value: 0.637047 Bottoms i-C4 i-C4 recovery: 98% i-C4 recovery value: 11.67
C3 condenser	280.43	31.01	205	0	Heat duty: –62970.85 BTU/h Mole fraction vapor: 33.33%. Mole fraction light liquid: 66.67%
C3 reboiler	405.29	22.65	207	0	Heat duty: 139586.31 BTU/h Mole fraction vapor: 38.91% Mole fraction light liquid 61.09%

4. Discussion

The glycol contactor operating conditions are driven by the input stream which is at 100°F and 970 psia with a pressure drop of 10 psi across the contactor and outlet temperature at the top of 100.02°F. The outcome of the simulation showed that water content was 6.96 lbm/MMscf which is less than the maximum required of 7 lbm/MMscf. The triethylene glycol from the contactor contains water and other hydrocarbon which are separated to obtain a more concentrated glycol for reuse. First, it is warmed by a reflux coil by 12.81°F and is greatly depressurized and cooled by the JT Valve (VLVE-100), by a pressure drop of 890 psia and a 8.78°F temperature drop. It then passes into the rich flash, which is a three-phase separator which separates the gas from the gas liquids from the water to produce three streams of natural gases, natural gas liquid and a mixture of triethylene glycol and absorbed water. From the rich flash, the triethylene glycol and water mixture passes through a cross exchanger where it was warmed by the heated liquid stream from the glycol reboiler and simultaneously cools the warming stream, resulting in 205.88°F rise in temperature of the triethylene and water stream, which moves into the glycol contactor where water is driven through the top outlet while mostly glycol falls to the bottom, where is passes into the reboiler for more heating. From the reboiler, mainly water and hydrocarbons are sent back to the glycol regenerator for recovery. Also, more concentrated triethylene glycol flows to the triethylene makeup from the reboiler, but first loses heat at the cross exchanger where it is cooled by 201.07°F as shown in Table 5, which also shows the glycol pump operates with a pressure drop of 965.3 psia due to flow and a 1.79°F rise in temperature with an efficiency of 68% and 38.17 hp.

The temperature, pressure and flow of the input stream conditions are 113.38°F and 955 psia and at 153.66 MMscfd (standard vapor volumetric flow), while there are two output streams. The first output product stream is fuel gas, predominantly methane, with about 63.5% mole of methane at 293 psia and 83°F with 153.46 MMscfd (standard vapor volumetric flow) while the other output product stream is a liquid stream. Unlike the first output product, it contains almost no methane of about 5.525e–06% mole and also serves as the input to the fractionation processing unit.

Table 6 shows that cooling occurred at the gas/liquid exchanger, gas/gas Exchanger and JT Valve by a temperature drop of 0.6°F, 59.6°F and 34.9°F respectively with pressure drop of 5 psia, 5 psia and 588 psia respectively, while cooling and warming simultaneously due to energy exchanges between the two streams, where heating occurs from stream 56 and cooling occur from Lean TEG stream. Separations of gas from natural gas liquids occurred in the cold separator and stabilizer, although separation is also possible in the flash vessel, which did not occur. The cold separator and stabilizer temperature and pressure drop are 0.2°F, 40°F and 2 psia, 2 psia, respectively. The reboiler supplies heat to the stabilizer with a temperature increase of 62.14°F which produces the final natural gas liquid stream, while the vapor from the stabilizer is recompressed by 288 psia and cooled by the air cooler by 169.7°F. Natural gas consisting mainly of methane was produced from the cold separator and warmed at the gas/gas exchanger by 68.4, after which is sent as fuel gas.

The natural gas liquid stream from the demethanizer was first sent to the deethanizer column. The feasible solution is when natural liquid from the demethanizer served as input to the depropanizer column which was isolated from the debutanizer column. The operation

of the depropanizer column is summarized in Table 7 with 34 stages, where input stream conditions are 376.91°F, 285 psia and 0.187 MMscfd (standard vapor flow). Across the depropanizer stages, temperature and pressure drops are 178.58°F and 2 psi respectively. The specification target includes a 99.9% recovery rate for propane which was fulfilled as indicated by the actual value of 99.9001%, while for the bottom product, the target for isobutane was 98% – it was not fulfilled as indicated by the actual recovery of 11.65%.

5. Conclusions

The project has been done successfully, with the water content reduced from 55.37 to 6.62 lbm/MMscf at the end of the dehydration processes, where the glycol liquid flow rate is 59.10 sgpm and temperature is 110.10°F and the conditions of the feed gas glycol contactor was 100°F, 970 psia with vapor flow of 190.07 MMscfd as shown in Figure 7. Recommendations for operations were fulfilled, lean glycol from the glycol pump followed the recommendation that its temperature should be 10°F greater than the input stream of the glycol contactors, and the glycol flow rate also exceeds the minimum recommended glycol flow of 2 sgpm.

In addition, from the depropanizer fractionation process, recovery are as follows C3: 99.9%; i-C4: 11.67%. The recovery of natural gas liquids depends on the composition of the natural gas, and the application of cooling by the exchangers, recycling of stream and conditions in the flash vessels, cold separators stabilizers and its reboilers and condensers.

References

[1] Leffler W.: *Natural gas liquids: A nontechnical guide*. PennWell Corporation, Oklahoma 2014.
[2] Devold H.: *Oil and gas production handbook: An introduction to oil and gas production transport, refining and petrochemical industry*. Edition 3.0, ABB Oil and Gas, Oslo, August 2013.
[3] Stewart M., Arnold K.: *Gas-liquids and liquid-liquid separators*. Elsevier, United Kingdom, 2008.
[4] Abdel-Aal H.K., Aggour M.A., Fahim M.A.: *Petroleum and Gas Filed Processing: Recovery, Separation and Fractionation of Natural Gas Liquids*. Marcel Dekker, New York 2003.
[5] Kidnay A.J., Parrish W.R.: *Fundamentals of natural gas processing*. Taylor and Francis Group, London 2006.

Journal of Geotechnology and Energy | vol. 38 | no. 1 | 2021 | pp. 27–34

Ewa Knapik

ORCID: 0000-0003-2808-1503
AGH University of Science and Technology in Krakow

Jerzy Stopa

ORCID: 0000-0001-6995-4249
AGH University of Science and Technology in Krakow

KINETIC MODELLING OF BIOSORPTION FOR HYDROCARBON REMOVAL FROM WASTEWATER USING A MODIFIED LOGISTIC EQUATION

Date of submission:
4.07.2021

Date of acceptance:
18.07.2021

Date of publication:
31.07.2021

https://journals.agh.edu.pl/jge

Abstract: The application of raw and modified biomass to remove hydrocarbons from wastewater by adsorption is a common practice. A mathematical modeling of biosorption kinetics is a crucial step to optimize the remediation process. In the present study, kinetic studies were carried out to describe the sorption process of crude oilon waste sunflower stalk pith. To increase sorption capacity, the pith surface was modified with polydimethylsiloxane (PDMS) and hydrophobic SiO_2 nanoparticles. The maximum loading of sorption for raw and hydrophobized material was 17.76 g/g and 19.62 g/g for crude oil, respectively. The system reached the equilibrium stage after 24 hours. The uptake profiles have been described by the pseudo-first order rate equation and the pseudo-second order rate equation. The calculated results were compared with experimental data and their fit was poor. To predict biosorption kinetics, a new mathematically efficient procedure based on a modified logistic equation was developed. The results indicate that the sunflower pith is an eco-friendly sorbent with significant potential for the removal of crude oil from water phase.

Keywords: kinetics, biosorption, oil spills, water treatment

1. Introduction

Natural fibers are useful for removing spills of crude oil and petroleum products from water surfaces. The applied sorbents should have high sorption capacity, selectivity, thermal and chemical stability, low cost of purchase and disposal. Fibers like kapok, barley straw, rice husks and residual leaves are often applied due to their wide availability and biodegradability [1]. Sorption capacity (the amount of adsorbate taken up by 1 g of sorbent) depends on many factors and varies from 1.1 g/g [2] for raw corn cobs up to 55 g/g for populus seed fibers [3]. The disadvantage of natural materials is their low selectivity towards oil. Advances in nanotechnology offer the opportunity to modify sorbents wettability relatively quickly and easily by the immobilization of controlled nanoparticles on the surface. In this way, plant fibers are used as a cheap filler and the introduced nanoparticles serve to improvetheir sorption properties (enhance the surface affinity to oil, enlarge the specific surface area of the sorbent). Currently, only few such hybrid materials are described in the literature. Wang et al. [4] have developed a super-hydrophobic sorbent based on kapok (*Ceibapentandra*) modified with magnetic nanoparticles of Fe_3O_4. The sorption capacity of the produced materialcompared to raw fibersincreased by 70.8% for n-hexane and 58.5% for toluene. The addition of magnetite not only changed the morphology of the surface of the fibers but also made the sorbent easier to remove from the water surface. Yang et al. [5] produced a sorbent based on coconut dust modified with nanoparticles of Fe_3O_4 and octadecylamine. This hybrid material was characterized by good sorption capacity of 8 g of petroleum/g, good selectivity and easy regeneration. A hybrid of nanoFe_3O_4-SiO_2-chitosan showed similar properties [6].

In this study, sunflower stem pith (parenchyma) was selected as a potential oil sorbent. The literature reports confirm good thermal, chemical and mechanical stability of this material. Annual production of sunflower parenchyma is estimated at 30–35 million tons and this plant is the fourth largest globally in terms of growing area [7]. Until now, it has not been considered as a sorbent material for the removal of oil from water bodies.

Studies on sorption kinetics help to understand the mechanism of the process, including the stages limiting the sorption rate. From a practical point of view, these measurements allow the determination of the maximum equilibrium sorption capacity (the amount of sorbent needed to remove a known amount of crude oil or its products). On their basis, it is also possible to determine the optimal time of sorbent contact with hydrocarbons. In the case of sorbents used to eliminate surface spills, an excessive prolongation of contact time may lead to the secondary release of hydrocarbons from the surface of the material due to the movement of sea waves. Over time, the mechanical stability of the sorbent may deteriorate due to mixing and swelling. In this work, both conventional kinetic models (pseudo-first order rate equation and the pseudo-second order rate equation) and a newly developed modified logistic equation were used to predict sorption kinetics of the tested material.

2. Method section

2.1. Materials

Raw sunflower stems were harvested from the Tarnów region, Poland, in 2017. The outer woody part of stems were removed in order to obtain the spongy pith. The material was then washed with distilled water and dried in an oven at 30°C until the moisture content decreased to 3% wt. For further experiments a fraction with particle size of 1.5–4.0 mm was used. Hydrophobic nanosilica was purchased from PlasmaChem GmbH. Polydimethylsiloxane from Acros Organics was used as a coupling agent. For sorption experiments a real crude oil from an oilfield in southern Poland was used.

2.2. Immobilization of SiO_2 nanoparticles on sunflower fibers by facile one-step spray method

10 g of PDMS was solved in 90 mL of n-pentane and 10 g of hydrophobic SiO_2 was dispersed in 100 mL of pure ethanol. Both solutions (10 mL of PDMS solution and 25 mL of dispersed SiO_2) were subsequently sprayed over the surface of 10 g of pith using a glass vaporizer from 25 cm distance. The prepared material was dried at 40°C for 6 hours. In further research the raw pith is denoted as material S and the modified pith as nS1.

2.3. Kinetics of adsorption

1 g of sorbent was contacted with 50 g of a crude oil in a 250 mL beaker at a specific time of contact (from 1 minute to 48 hours). After the specific time elapsed, the sorbent was removed from the oil using steel sieves (1 mm mesh holes). Dripping for 10 minutes allows for

a complete drainage of the excess of liquid, the remaining sorbent was weighed. Sorption capacity q_t at time t was calculated according to equation:

$$q_t = \frac{m_t - m_s}{m_s} \tag{1}$$

where m_t and m_s are the mass of the wet and dry sorbent, respectively [g].

2.4. Modelling approach

The mathematical description was based on the pseudo-first-order equation and the pseudo-second-order equation. The pseudo-first order (PFO) model is shown by equation:

$$\frac{dq_t}{dt} = K_1(q_e - q_t) \tag{2}$$

where q_t and q_e are the amount of oil adsorbed by sunflower pith at time t and at equilibrium, respectively [g/g] and K_1 is the rate constant of the pseudo-first order model [1/min]. For the boundary conditions of $q_t = 0$ at $t = 0$ the pseudo-first order model after integrating follows the equation:

$$\ln(q_e - q_t) = \ln q - K_1 t \tag{3}$$

This equation, developed originally by Lagergren, described the kinetics of carboxylic acids sorption on charcoal [9]. Oil sorption on acetylated corn cobs was also well described by this equation [10]. It is assumed that this PFO model well predicts the initial stage of the process before reaching equilibrium [11].

The pseudo-second-order (PSO) kinetic model is expressed as:

$$\frac{dq_t}{dt} = K_2(q_e - q_t)^2 \tag{4}$$

where K_2 refers to the adsorption rate constant of PSO kinetic model. This equation can be integrated for initial condition $q_t = 0$ at $t = 0$ and described according to:

$$\frac{t}{q_t} = \frac{1}{K_2 q_e^2} + \frac{t}{q_e} \tag{5}$$

In the oil-biosorbent system this kinetic equation was used to model sorption of diesel oil on rice husk [12], crude oil on acetylated pineapple leaves [13], gasoline on carbon nanotubes [14].

Płaziński and Rudziński [15] showed that both of the abovementioned equations (PSO and PFO) are empirical equations to which no specific physical models correspond. Fitting experimental data to these models does not explain the mechanism of the process. The logistic equation provides more information about interactions in studied systems. Çelekli et al. applied successfully the logistic model to describe kinetic sorption of Reactive Red 120 on *C. contraria* [16] and *Moringaoleifera* seed [17]. The applied equation allowed to explain the physical nature of the sorption and precisely predict the maximum sorption capacity. In this study, the authors used a modified logistic equation in the form:

$$\frac{1}{q_t}\frac{dq_t}{dt} = F(t)(q_e - q_t) \tag{6}$$

where $F(t)$ is a function of time and can be given in the form:

$$F(t) = \frac{k_{l_g}}{t^{\alpha}} \tag{7}$$

where k_{lg} is an adsorption rate constant [–] and α is a constant describing sorbent-sorbate interactions, α = 0.5 was assumed in the work. After integration within the boundaries with the initial condition $q_{t\to\infty} - q_e$ the solution of equation (7) can be written as follows:

$$q_t = \frac{q_e}{1 + C \cdot \exp\left(\frac{-q_e \cdot k_{l_g}}{1-\alpha} \cdot t^{1-\alpha}\right)} \tag{8}$$

where C is the model constant. The parameters q_e, k_{lg}, C, and α were fitted to the experimental values by use of the least squares method.

RMSE (root mean square error) and χ^2 statistical criteria were applied to compare the measured and calculated results of sorption kinetics for oil sorption onto biomass. These parameters were calculated as follows:

$$RMSE = \sqrt{\frac{1}{N}\sum_{i=1}^{N}(q_{e,\exp} - q_{e,\text{calc}})^2} \tag{9}$$

$$\chi^2 = \sum_{i=1}^{N}\frac{(q_{e,\exp} - q_{e,\text{calc}})^2}{q_{e,\text{calc}}} \tag{10}$$

where N is the data numbers, $q_{e,\exp}$ and $q_{e,\text{calc}}$ are the empirical and calculated values, respectively.

3. Results and discussion

The contact time significantly influences oil sorption capacity for both raw and modifiedpith sorbents as shown in Figure 1. Values of parameters fitted to the kinetic models are given in Table 1.

The sorption capacity increases with time and in the initial stage the relative sorption rate is high. After 24 hours crude oil uptakes attain equilibrium. The specific surface area of the sorbent plays a key role in the first stage of process while the spongy structure of pith determines its high sorption capacity for longer contact times. After 15 minutes of contact, raw sunflower fiber sorbs of 9.03 g of crude oil, while modified material with an increased surface area sorbs 13.79 g/g. Finally, the maximum sorption loading for the tested oil is 17.76 g/g and 19.62 g/g for materials S and nS1, respectively. The structure and composition of the sorbent affect the time after which the maximum sorption capacity is reached. For hydrophobic nanopowders the equilibrium state is attained quickly. The optimum contact time for carbon nanotubes [18] and hydrophobized aluminium nanoparticles is 30 minutes [19]. Plant sorbents (highly fragmented, fibrous and hydrophobized with various chemical additives) are equally effective and achieve maximum absorbency in several minutes. Sugar cane pulp modified with stearic acid [20] and acetylated rice husks [21] reached the equilibrium after 15 minutes. Materials with a complex porous structure such as luffa fruits [22], kapok fibers [22] or polyurethane foams [23] require a longer contact time, up to 24 hours.

The adsorption is faster and more effective for modified material than for raw fibers. Even at very short contact time, less than 1 minute, the tested materials show rather a high sorption capacity of 8 g/g.

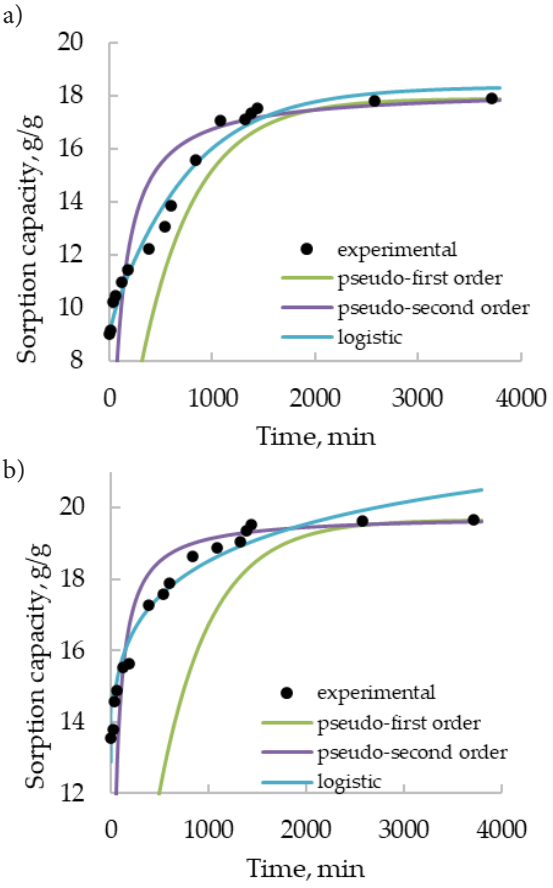

Fig. 1. Kinetics of crude oil sorption for: a) unmodified; b) modified pith

Table 1. Kinetic parameters for the removal of crude oil by raw and hydrophobized pith

Model	Parameters	Raw pith	Hydrophobized pith
Pseudo-first order	K_1 [1/min]	0.0019	0.0019
	q_e [g/g]	17.90	19.67
	χ^2	2678	5521
	RSME	5.164	8.089
Pseudo-second order	K_2 [g/(g*min)]	0.0006	0.0014
	q_e [g/g]	18.25	19.80
	χ^2	415.159	321.886
	RSME	3.370	4.108
Modified logistic	q_e [g/g]	18.824	19.932
	k_{lg}	0.002	0.002
	C	1.336	0.553
	αA	0.5	0.5
	χ^2	0.537	0.067
	RSME	0.681	0.262
Maximum sorption capacity determined experimentally	q_{exp} [g/g]	17.757	19.619

Table 2. Comparison of kinetic models for adsorption of oil on hydrophobized plant sorbents

Model	Parameters	Adsorbent – adsorbate		
		Enzyme-modified corn stalk – crude oil [24]	Acetylated *Dacryodes edulis* leaf – crude oil [25]	Kapok modified with $PBMA/SiO_2$ – oil 150SN [26]
Pseudo-first order	K_1 [1/min]	0.840	0.251	3.582
	$q_{e,calc}$ [g/g]	22.744	4.846	75.700
	χ^2	2.574	0.019	0.441
	RSME	2.261	0.112	2.166
Pseudo-second order	K_2 [g/(g · min)]	0.019	0.102	0.071
	$q_{e,calc}$ [g/g]	25.575	5.064	78.683
	χ^2	6.565	0.004	0.938
	RSME	2.419	0.048	2.859
Modified logistic	k_{lg}	0.009	0.092	0.012
	$q_{e,calc}$ [g/g]	25.410	4.927	77.246
	C	1.023	2.848	0.681
	α	0.5	0.5	0.5
	χ^2	0.045	0.003	0.065
	RSME	0.313	0.049	0.837
Maximum sorption capacity determined experimentally	q_{exp} [g/g]	24.98	4.990	78.43

The pseudo-first order model is ineffective when describing the sorption of oil on the tested sorbents. The mathematical model should fit the measurement data in their entire range. PSO and PFO models poorly describe the initial stage of sorption (for short contact times) as shown in Figure 1. Based on the χ^2 and *RSME* values it can be seen that the discrepancies between the predictions of both models and the actual data are quite large. A modified logistic model provides the best match to the experimental data.

The developed logistic model was fitted to experimental data reported by other researchers to prove its applicability in kinetics modelling. Table 2 summarizes the kinetic parameters of selected hydrophobized plant sorbents.

In general, in most works, the pseudo-second order model gives a better fit than the pseudo-first order equation, and it predicts well the maximum sorption capacity in particular. The newly developed kinetic model describes well the data over the entire measuring range and can be used for different fibers.

4. Conclusions

Mathematical modelling of the adsorption process allows the identification of the process mechanisms (kinds of interactions between the sorbent and the sorbate) and to predict its course in time. Since the chemical compositions of both crude oil and natural fibers are complex, the most appropriate mathematical model should be fitted separately to each tested system. The sorption capacity is 17.76 and 19.62 g oil/g for raw and modified pith, respectively. The sorption equilibrium time is 24 hours due to the porous structure of the pith. The commonly used kinetics models (pseudo-first order and pseudo-second order equations) do not allow for an accurate prediction of sorption capacity for hydrocarbons in the whole measurement range. Due to the complex structure of the studied sorbents, the typical kinetic description was not sufficient, and a modified logistic equation was proposed. The calculations based on this concept showed that this model closely agreed with the experimental results.

Author Contributions: conceptualization, E.K., J.S.; methodology, J.S.; software, J.S.; validation, E.K., and J.S.; formal analysis, E.K.; investigation, E.K.; resources, J.S.; data curation, E.K.; writing – original draft preparation, E.K.; writing – review and editing, E.K.; visualization, E.K.; supervision, J.S.; project administration, J.S.; funding acquisition, J.S. All authors have read and agreed to the published version of the manuscript.

References

[1] Wahi R., Chuah L.A., Choong T.S.Y., Ngaini Z., Nourouzi M.M.: *Oil removal from aqueous state by natural fibrous sorbent:An overview*. Separation and Purification Technology, vol. 113, 2013, pp. 51–63, https://doi.org/10.1016/j.seppur.2013.04.015.

[2] Dashti N., Ali N., Khanafer M., Radwan S.S.: *Oil uptake by plant-based sorbents and its biodegradation by their naturally associated microorganisms*. Environmental Pollution, vol. 227, 2017, pp. 468–475, https://doi.org/10.1016/j.envpol.2017.04.089.

[3] Likon M., Rem M., Ducman V., Svegl F.: *Populus seed fibers as a natural source for production of oil super absorbents*. Journal of Environmental Management, vol. 114, 2013, pp. 158–167, https://doi.org/10.1016/j.jenvman.2012.03.047.

[4] Wang J., Geng G., Liu X., Han F., Xu J.: *Magnetically superhydrophobic kapok fiber for selective sorption and continuous separation of oil from water*. Chemical Engineering Research and Design, vol. 115, 2016, 122–130, https://doi.org/10.1016/j.cherd.2016.09.032.

[5] Yang L., Wang Z., Yang L., Li X., Zhang Y., Lu C. *Coco peat powder as a source of magnetic sorbent for selective oil – water separation*. Industrial Crops and Products, vol. 101, 2017, pp. 1–10, https://doi.org/10.1016/j.indcrop.2017.02.040.

[6] Soares F.S., Rodrigues M.I., Trindade T., Daniel-da-Silva A.L.: *Chitosan-silica hybrid nanosorbents for oil removal from water*. Colloids and Surfaces A: Physicochemical and Engineering Aspects, vol. 532, 2017, pp. 305–313, https://doi.org/10.1016/j.colsurfa.2017.04.076.

[7] Fortunati E., Luzi F., Jiménez A., Gopakumar D.A., Puglia D., Thomas S., Kenny J.M., Chiralt A., Torre L.: *Revalorization of sunflower stalks as novel sources of cellulose nanofibrils and nanocrystals and their effect on wheat gluten bionanocomposite properties*. Carbohydrate Polymers, vol. 149, 2016, pp. 357–368, https://doi.org/10.1016/j.carbpol.2016.04.120.

[8] Abou-Elela S.I., Ali M.E.M., Ibrahim H.S.: *Combined treatment of retting flax wastewater using Fenton oxidation and granular activated carbon*. Arabian Journal of Chemistry, vol. 9, 2016, pp. 511–517, https://doi.org/10.1016/j.arabjc.2014.01.010.

[9] Lagergren S.: *About the theory of so-called adsorption of soluble substances*. Kungliga Svenska Vetenskapsakademiens Handlingar, vol. 24, 1898, pp. 1–39.

[10] Nwadiogbu J.O., Ajiwe V.I.E., Okoye P.A.C.: *Removal of crude oil from aqueous medium by sorption on hydrophobic corncobs: Equilibrium and kinetic studies*. Journal of Taibah University for Science, vol. 10, 2016, pp. 56–63.

[11] Tan K.L., Hameed B.H.: *Insight into the adsorption kinetics models for the removal of contaminants from aqueous solutions*. Journal of the Taiwan Institute of Chemical Engineers, 2017, vol. 74, pp. 25–48, https://doi.org/10.1016/j.jtice.2017.01.024.

[12] Wang Z.; Barford J.P., Wai C., Mckay G.: *Kinetic and equilibrium studies of hydrophilic and hydrophobic rice husk cellulosic fibers used as oil spill sorbents*. Chemical Engineering Journal, vol. 281, 2015, pp. 961–969, https://doi.org/10.1016/j.cej.2015.07.002.

[13] Chin S., Kong H., Tien S., Johari K., Saman N., Azizi M., Yunus C., Mat A.: *Separation of dissolved oil from aqueous solution by sorption onto acetylated lignocellulosic biomass – equilibrium, kinetics and mechanism studies*. Journal of Environmental Chemical Engineering, vol. 4, 2016, pp. 864–881, https://doi.org/10.1016/j.jece.2015.12.028.

[14] Kayvani A., Mckay G., Manawi Y., Malaibari Z., Hussien M.A.: *Outstanding adsorption performance of high aspect ratio and super-hydrophobic carbon nanotubes for oil removal*. Chemosphere, vol. 164, 2016, pp. 142–155, https://doi.org/10.1016/j.chemosphere.2016.08.099.

[15] Płaziński W., Rudziński W.: *Kinetyka adsorpcji na granicy faz roztwór/ciało stałe. Znaczenie równań pseudo-first order oraz pseudo-second order*. Wiadomości Chemiczne, vol. 65, 2011, pp. 1055–1067.

[16] Çelekli A., Yavuzatmaca M., Bozkurt H.: *An eco-friendly process: Predictive modelling of copper adsorption from aqueous solution on Spirulina platensis*. Journal of Hazardous Materials, vol. 173, 2010, pp. 123–129, https://doi.org/10.1016/j.jhazmat.2009.08.057.

[17] Çelekli A., Al-Nuaimi A.I., Bozkurt H.: *Adsorption kinetic and isotherms of Reactive Red 120 on Moringa oleiferaseed as an eco-friendly process*. Journal of Molecular Structure, vol. 1195, 2019, pp. 168–178, https://doi.org/10.1016/j.molstruc.2019.05.106.

[18] Kayvani A., Rhadfi T., Mckay G., Al-Marri M., Abdala A., Hilal N., Hussien M.A.: *Enhancing oil removal from water using ferric oxide nanoparticles doped carbon nanotubes adsorbents*. Chemical Engineering Journal, vol. 293, 2016, pp. 90–101, https://doi.org/10.1016/j.cej.2016.02.040.

[19] Franco C.A., Cortés F.B., Nassar N.N.: *Adsorptive removal of oil spill from oil-in-fresh water emulsions by hydrophobic alumina nanoparticles functionalized with petroleum vacuum residue*. Journal of Colloid and Interface Science, vol. 425, 2014, pp. 168–177, https://doi.org/10.1016/j.jcis.2014.03.051.
[20] Said A.E.A.A., Ludwick A.G., Aglan H.A.: *Usefulness of raw bagasse for oil absorption: A comparison of raw and acylated bagasse and their components*. Bioresource Technology, vol. 100, 2009, pp. 2219–2222, https://doi.org/10.1016/j.biortech.2008.09.060.
[21] Wang Z., Barford J.P., Wai C., Mckay G.: *Kinetic and equilibrium studies of hydrophilic and hydrophobic rice husk cellulosic fibers used as oil spill sorbents*. Chemical Engineering Journal, vol. 281, 2015, pp. 961–969, https://doi.org/10.1016/j.cej.2015.07.002.
[22] Annunciado T.R., Sydenstricker T.H.D., Amico S.C.: *Experimental investigation of various vegetable fibers as sorbent materials for oil spills*. Marine Pollution Bulletin, vol. 50, 2005, pp. 1340–1346, https://doi.org/10.1016/j.marpolbul.2005.04.043.
[23] Santos O.S.H., Coelho da Silva M., Silva V.R., Mussel W.N., Yoshida M.I.: *Polyurethane foam impregnated with lignin as a filler for the removal of crude oil from contaminated water*. Journal of Hazardous Materials, vol. 324, 2017, pp. 406–413, https://doi.org/10.1016/j.jhazmat.2016.11.004.
[24] Peng D., Ouyang F., Liang X., Guo X., Dang Z., Zheng L.: *Sorption of crude oil by enzyme-modified corn stalk vs. chemically treated corn stalk*. Journal of Molecular Liquids, vol. 255, 2018, pp. 324–332, https://doi.org/10.1016/j.molliq.2018.01.178.
[25] Nnaji N.J.N., Onuegbu T.U., Edokwe O., Ezeh G.C., Ngwu A.P.: *An approach for the reuse of Dacryodes edulis leaf: Characterization, acetylation and crude oil sorption studies*. Journal of Environmental Chemical Engineering, vol. 4, 2016, pp. 3205–3216, https://doi.org/10.1016/j.jece.2016.06.010.
[26] Wang J., Zheng Y., Kang Y., Wang A.: *Investigation of oil sorption capability of PBMA/SiO_2 coated kapok fiber*. Chemical Engineering Journal, vol. 223, 2013, pp. 632–637, https://doi.org/10.1016/j.cej.2013.03.007.

Journal of Geotechnology and Energy | vol. 38 | no. 1 | 2021 | pp. 35–40

Olga Likhacheva

ORCID: 0000-0001-6580-0787
Udmurt State University, Izhevsk, Russian Federation

Gleb Kashin

ORCID: 0000-0002-8620-907X
Gazpromneft STC, Tyumen, Russian Federation

Vadim Mironychev

ORCID: 0000-0002-1018-6078
Udmurt State University, Izhevsk, Russian Federation

THE USE OF PASSIVE SEISMIC EXPLORATION TO IDENTIFY OIL-BEARING RESERVOIRS IN THE UDMURT REPUBLIC (RUSSIA)

Date of submission:
22.05.2021

Date of acceptance:
22.06.2021

Date of publication:
31.07.2021

https://journals.agh.edu.pl/jge

Abstract: The level of oil production in the Udmurt Republic is currently experiencing a declining trend due to the depletion of large and medium-sized oil fields that have been in operation for a long time. Therefore, the main challenge in this region is to stabilize & increase oil extraction by means of exploring more promising oil fields of a smaller size. However, some issues cause difficulties. Firstly, 2D and 3D seismic data often do not provide the reliable mapping of small fields. Secondly, geological prospecting and exploration, along with exploratory drilling, make these works costly. Furthermore, the estimation of the reserves for such deposits often contains errors. Passive seismic exploration is proposed as a solution to these problems, reducing exploratory and exploitation drilling costs, with the time required for geological exploration also being diminished.

Keywords: passive seismic, Udmurt Republic, small-sized reservoir, oil and gas

1. Introduction

Rapid crude oil depletion is picking up speed in the Udmurt Republic, with a production rate decrease being common at all long-term operational oil fields of large and medium size. Therefore, the main challenge in this region is to stabilize and increase the amount of oil extraction by exploring the potentially more prospective small fields.

The oil fields of the Udmurt Republic contain nearly 6.4 billion barrels of proven reserves. Successfully discovered oil fields may supply the region with potential resources of up to 9.6 billion barrels [1].

Oil fields discovered in the region in 2017 have substantiated good prospects of searching for new hydrocarbon deposits in the Udmurt Republic. They included the Vesenny, Pikhtovsky, and Aleksandrovsky fields [2]. Besides, there are geological exploration works in progress in the Orosovsky and Vyazovsky fields.

The geological complexity of structures and considerable heterogeneity of facies formations leads to difficulties in converting theoretical resources into producible reserves. The most promising geological structures are small-sized reservoirs containing fewer than 2.1 million barrels of original oil in place (OOIP). However, it is often challenging to detect such structures using traditional exploratory methods because of some problems, complicated the process.

The exploration of the Oparinsky oil field, located in the Udmurt Republic (Fig. 1a), using a traditional set of works, was aimed at prospecting small reservoirs, but it became an example of ineffectiveness. The field was estimated to hold 6.3 million barrels of OOIP and 312,000 barrels of recoverable reserves. However, 10 of the 11 wells drilled turned out to be empty. Based on the data received from geological prospecting works, the Oparinsky field was reevaluated as having 312,000 barrels of OOIP and 64,000 barrels of recoverable reserves (Fig. 1b). Well drilling at the Oparinsky field alone cost $22 million (Tab. 1).

Problems which typically complicate the exploration and operation of small-sized reservoirs include:

- lithological and geological complexity of such structures;
- difficulties in proper detection of small-sized reservoirs having a limited number of prospecting and exploratory wells;
- errors during the reserves' calculation process and uncertainties in proper locating of exploratory wells;
- difficulties in detecting reservoirs of small size based on the 2D and 3D seismic data;
- costly prospecting, exploratory and exploitation drilling.

a)

b)

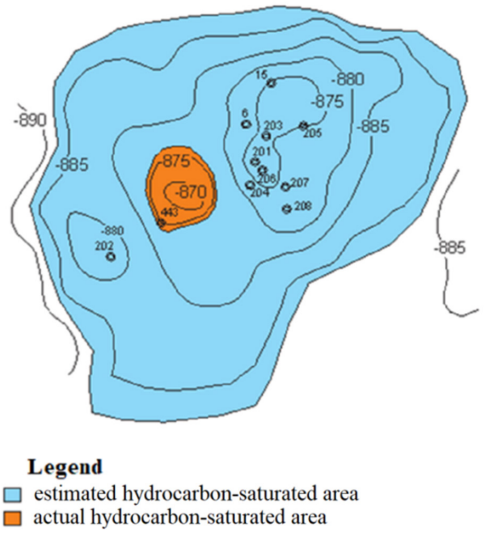

Fig. 1. Location of the Oparinsky field (a); structural map of the Oparinsky field (b), showing estimated and actual hydrocarbon saturated zones

Table 1. Results of prospecting and exploratory drilling at the Oparinsky field

No.	Parameter name	Parameter value
1	Estimated reserves (before prospecting drilling) [thousand bbls]	6 319
2	Original oil in place (OOIP) [thousand bbls]	312.4
3	Recoverable reserves [thousand bbls]	63.9
4	The number of wells	11
5	The number of empty wells	10
6	Well drilling cost [million USD]	22

Passive seismic exploration is proposed as a solution to these problems. The use of this technology could reduce the amount of time required for hydrocarbon exploration and enable a reduction of the exploration and development costs.

2. Method section

Passive seismic exploration uses low frequencies as seismic sources. This technique makes it possible to give the correct forecast for the discovery of oil and gas accumulated in reservoirs. 3D seismic is applied to detect geological structures, having good prospects [3, 4], while the passive seismic data confirms the hydrocarbon presence with precision. The main feature of passive seismic exploration is the specific nature of the low-frequency seismic signals, carrying valuable geological information in the subsurface [5]. These signals are produced by the oil- and gas-bearing reservoir rather than reflected or refracted by the layer's surface (Fig. 2).

3. Examples

In the Udmurt Republic, passive seismic exploration was applied in a variant of the "ANCHAR" method in 1999. The territory of implementation included the Debyosy, Eastern Tylovay fields, and Mar'inskaya structure (Fig. 3). The aim was to detect and estimate geological structures for the subsequent prospecting and exploration work planning. The use of "ANCHAR" technique in the Debyosy, Eastern Tylovay fields and Mar'inskaya structure allowed it to be determined that fluid contacts of reservoirs did not correspond with the subsurface structures, which were detected by 3D seismic exploration and exploration well drilling. Locations for further deep-well drilling were selected according to passive seismic data [6].

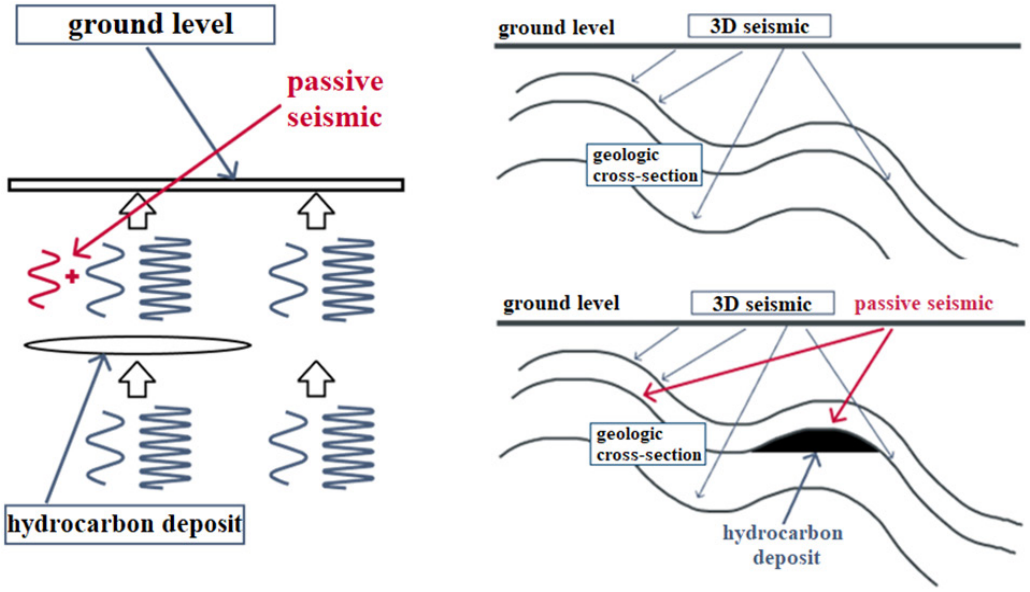

Fig. 2. Passive seismic principles

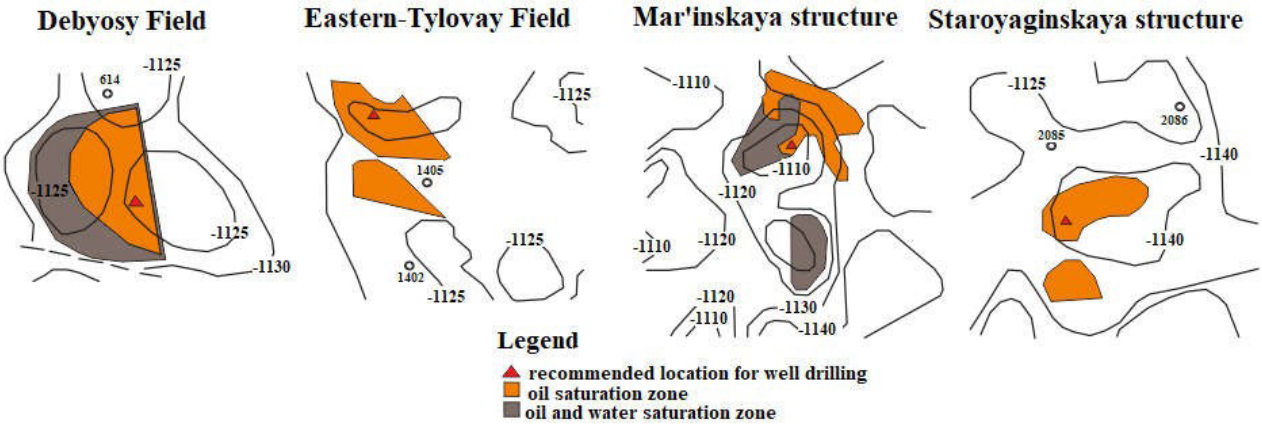

Fig. 3. Estimated hydrocarbon saturation of the Debyosy, Eastern Tylovay fields, Mar'inskaya, Staroyaginskaya structures, according to the "ANCHAR" method

Passive seismic exploration may become a way to detect previously missed oil-bearing reservoirs. An exploration of the Staroyaginskaya geological structure with the use of "ANCHAR" method enabled the identification of hydrocarbons accumulated in a synclinal part of the structure (Fig. 3). Based on the obtained results, oil and gas saturation of this structure was forecast, and more proper locations for exploration well drilling were recommended. Hydrocarbon accumulation in synclines is uncommon in the Udmurt Republic. Without the data provided by the "ANCHAR" method, this oil-bearing structure would have been missed.

Passive seismic exploration, in combination with traditional exploratory methods, provides a forecast of hydrocarbon saturation. Reduction of the number of empty wells achieved using passive seismic exploration can decrease the amount of time required for field exploration [7]. Hence, it results in economical expenses for exploration and exploitation works.

The lack of accurate mapping and costly exploratory drilling makes it unprofitable to discover fields with less than 2 million barrels of OOIP, but passive seismic exploration can address this issue. Also, small-sized reservoirs and non-structural traps of complex geology can be explored by means of passive seismic, with their oil and gas saturation being forecast. Moreover, this technology serves for detecting fluid contacts which do not correspond with the subsurface structures.

There are nearly two hundred promising oil fields of small and tiny size that have been discovered in the Udmurt Republic. The north-eastern part of the region has 65 such oil fields (Fig. 4). The estimated OOIP of these fields are shown in Table 2.

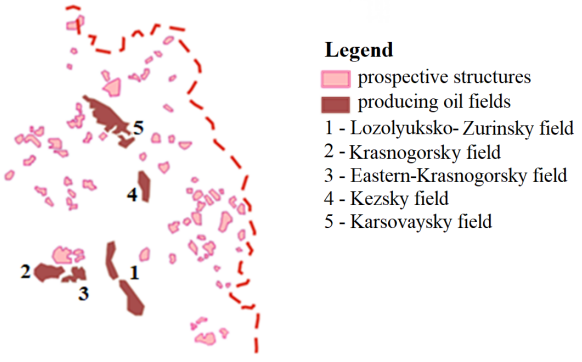

Fig. 4. Prospective structures located in the north-eastern part of the Udmurt Republic

The projects using passive seismic have been effectively implemented for geological prospecting and exploration of various production areas in the Volga-Ural Petroleum Province, including Melekess, Buzuluk depressions and Kama, Zhigulevsko-Orenburg, Tatar, Sol-Iletsk arches. This technology has improved the chance of the success of exploration wells by up to 85%. The depth of the accurately explored zone was 400 m to 7 000 m [5, 8].

Table 2. Estimated oil reserves of 65 perspective structures

No.	Parameter name	Parameter value
1	Estimated OOIP [million bbls]	1 420–1 775
2	Recoverable reserves [million bbls] (recovery factor is 0.35)	497–618
3	Estimated cost of recoverable reserves [billion USD] ($35/bbl)	17–22

4. Conclusions

1. Due to the depletion of large oil fields in the Udmurt Republic, more attention is being paid to the development of very small ones containing significant hydrocarbon reserves. However, detecting them is extremely difficult in the case of a traditional techniques.
2. Success in the exploration and production of well drilling depends on accurate geological model and a clear delineation of the reservoir. The results of the first well drilling largely determine the fate of oil field.
3. Proper detection of small-sized reservoirs may be much more difficult without data received by passive seismic exploration works.
4. This exploration technique of finding hydrocarbons uses low frequencies as the seismic sources. The main purpose of the method is to discern the geological structures that have good prospects.
5. Passive seismic may be applied to find the most appropriate locations for proposing and exploration well drilling with the further use of these wells as production ones during the subsequent process of oilfield development. This will make the operation of very small fields much more profitable.
6. Passive seismic exploration provides a correct forecast for the discovery of hydrocarbon reservoirs occupying structurally complicated small-sized and non-structural traps. Also, such an exploration method allows the fluid contacts of deposits to be detected if they do not correspond with the subsurface structure.
7. The proposed technology can also be successfully applied to already discovered and exploited oil fields in order to determine accurate reservoir oil-water contact as well as to monitor the process of development.

8. Passive seismic surveys may be conducted further at regular intervals during the oilfield development to control the conditions of hydrocarbon reservoirs. It will rationalize the process of oilfield development, increasing the productivity index.
9. Passive seismic exploration may not only be applied in the Udmurt Republic but also in other regions all over the world with success. This technique can enable valuable exploration information to be obtained, regardless of geological structure complexity and reservoir depth, for oil fields located anywhere in the world.

Author Contributions: conceptualization, G.K.; methodology, V.M.; software, G.K.; validation, G.K., O.L., V.M.; formal analysis, O.L.; investigation, G.K.; resources, G.K.; data curation, V.M.; writing – original draft preparation, G.K., O.L.; writing – review and editing, O.L.; visualization, O.L.; supervision, V.M.; project administration, G.K.; funding acquisition, G.K., O.L. All authors have read and agreed to the published version of the manuscript.

References

[1] Savel'yev V.A.: *Neftegazonosnost' i perspektivy osvoeniya resursov nefti Udmurtskoy Respubliki* [Oil and gas potential and prospects of oil resources development in the Udmurt Republic]. Institut komp'yuternykh issledovaniy [Institute of computer research], Izhevsk–Moscow 2003.
[2] JSC Udmurtneft: www.udmurtneft.ru/news/5618 [5.05.2019].
[3] Bondarev I.V.: *Seysmorazvedka MOGT. Kurs lektsiy dlya bakalavrov. Chast' 3. Osnovnye teorii, metodiki polevykh rabot i obrabotki rezul'tatov seysmicheskikh nablyudeniy metodom obshchey glubinnoy tochki* [Seismic MCDP. Course of lectures for bachelors. Part 3. Basic theories, methods of field work and processing of seismic observations by the method of common depth point]. Yekaterinburg, Publ. UGGGA, 1996.
[4] Gritsenko S.A.: *Izobrazhenie geologicheskikh razrezov i opredelenie skorostey metodom obshchey glubinnoy tochki* [Image of geological sections and determination of velocities by the method of Common depth point]. FGBOU "VSEGEI", St. Peterburg 2014.
[5] Acoustic low-frequency exploration scientific and technological complex: anchar.ru [10.05.2019].
[6] Arutyunov S.L.: *Otchet o vypolnenii opytnykh rabot metodom nizkochastotnoy razvedki ANChAR na territorii Udmurtskoy Respubliki* [Report on the implementation of experimental work by the method of low-frequency intelligence ANCHAR on the territory of the Udmurt Republic]. Dogovor A-39/99 ot 2.07.1999 *g* [Agreement A-39/99 of 2.07.1999], Orenburg–Izhevsk 1999.
[7] Lysenko V.D.: *Innovatsionnaya razrabotka neftyanykh mestorozhdeniy* [Innovative development of oil fields]. OOO "Nedra – Biznestsentr", Moscow 2000.
[8] Sharapov I.R., Shabalin N.Yu., Biryaltsev E.V., Feofilov S.A., Ryzhov V.A.: *Innovacionnye metody nizkochastotnoj sejsmorazvedki v neftegazovoj promyshlennosti – opyt primeneniya v Rossii* [Innovative passive microseismic methods in oil and gas industry – experience applied in Russia]. Materials of the International Scientific Geological Conference "AtyrauGeo-2015", 2015.

Journal of Geotechnology and Energy | vol. 38 | no. 1 | 2021 | pp. 41–46

Mykhailo Myslyuk

ORCID 0000-0003-3952-1316
Institute of Petroleum Engineering, Ivano-Frankivsk National Technical University of Oil and Gas, Ivano-Frankivsk, Ukraine

Ruslan Dolyk

ORCID 0000-0001-9187-4659
Institute of Petroleum Engineering, Ivano-Frankivsk National Technical University of Oil and Gas, Ivano-Frankivsk, Ukraine

RISK ASSESSMENT OF PACKED HOLEASSEMBLIES FOR ROTARY WELL DRILLING

Date of submission:
21.06.2021

Date of acceptance:
30.06.2021

Date of publication:
31.07.2021

https://journals.agh.edu.pl/jge

Abstract: The main elements of the statistical model of packed hole assemblies (PHA) design for drilling holding sections in conditions of information uncertainty are formalized and described. A constraint system has been given for the angle maintenance conditions of wellbore direction and dynamic stability of bottom hole assembly (BHA) lateral vibrations.

The influence of the information uncertainty of some factors (angle, parameters of the drilling practice, presence of local caverns, etc.) on risk indicators has been analyzed according to the results of the numerical calculations. It has been determined that the risks of angle maintenance disturbance are significantly influenced by the angle and weight on the bit (WOB), and dynamic stability conditions, such as angle and rotation frequency.

Risks of multi-supported BHAs which have been designed for conditions of minimizing bit side force, dynamic stability and include 4–6 stabilizers.

Keywords: information uncertainty, bottom hole assembly (BHA), holding section, stabilizer, risks, statistical decision-making model, static and dynamic characteristics

1. Introduction

Improving the efficiency of the drilling of oil and gas wells requires an integrated approach regarding the choice of technological solutions aimed at ensuring the design parameters and quality of the trajectory, preventing complications and accidents, achieving high technical and economic indicators, etc. In this aspect, one of the important technological solutions is the design of bottom hole assemblies (BHA). The trajectory of the well with maintained angle and shape of well cross-sectionin the form of a circle are considered to be one of the most basic requirements of high-quality casing cementing [1].

2. BHA selection model

Currently in engineering practice BHA design for drilling holding sections is substantiated mainly on the basis of the analysis of static solutions of differential equations of elastic axis equilibrium of drilling string bottom, usually for a plane design scheme [2–5]. Considerable attention is paid to the investigation and design of multi-supported PHA taking into account lateral vibrations and dynamic stability of the drilling string bottom [5–7].

An important direction for BHA design is the use of decision-making models with a flexible choice of optimality criterion and taking into account information uncertainty about input data (angle, parameters of the drilling practice, presence of local caverns, etc.) [8, 9]. The methods of BHA multicriteria efficiency estimation for static and dynamic characteristics are being developed [9] which are determined by technological requirements and the need for field data about the influence of drilling practice on wellbore quality in appropriate well drilling conditions.

In general, the design of PHA is carried out by taking into account the multifunctional requirements that determine BHA effectiveness depending on technical, technological and natural factors. Since the number of factors affecting the angle maintenance and drilling parameters are random, BHA design in some of their class ϑ should be justified by a statistical decision-making model [9]:

$$\begin{cases} R(p^{\nu}, c^{\nu}) \to \min,\ \nu \in \vartheta,\ p^{\nu} \in D^{\nu} \\ \varphi(p^{\nu}) \le 0 \end{cases} \tag{1}$$

where:

$R(p^{\nu}, c^{\nu})$ – a risk ν^{th} BHAof class of ϑ layouts,

$p^{\nu} = (p_1^{\nu}, p_2^{\nu}, ..., p_n^{\nu})^{\mathrm{T}}$ – the vector of variable parameter of the ν^{th} BHA with the definition area D^{ν},

$c^{\nu} = (c_1^{\nu}, c_2^{\nu}, ..., c_m^{\nu})^{\mathrm{T}}$ – the vector of known parameters,

$\varphi(p^{\nu})$ – the constraints system for the BHA parameters.

The system defines limitations on drilling practice parameters, geometric parameters and stiffness of the BHA elements, their static and dynamic characteristics in order to ensure the efficiency and quality of well drilling. The latter constraints are built on the basis of the field data analysis in similar drilling conditions [9].

The model (1) with constraint system $\varphi(p^{\nu})$ allows a multicriteria assessment of BHA variants and takes into account the information uncertainty of some parameters (angle, drilling practice parameters, presence of local caverns, etc.). The presence of local caverns is simulated by the absence of contact of one (and arbitrary) stabilizers with the wellbore wall. For given geological and technical conditions, alternative variants class ϑ is formed depending on the structural features, geometrical and technical parameters, number and placement of the BHA elements.

Risk function $R(p^{\nu}, c^{\nu})$ indicates the probability of violating the constraint system for static and dynamic BHA characteristics due to inaccurate information of the decision-making model (1).

Static characteristics include bit side force F_B, inclination angle ψ of bit axis to well axis, reaction R_i on stabilizers, contact point coordinate L of drill collar (DC) with wellbore wall and dynamic characteristics – natural frequency, amplitude-frequency characteristics, and others [2–11]. The risks of BHA alternative variants are estimated using the method of statistical simulation (Monte Carlo).

It should be noted that risk management depends on the formalization of the BHA designing task (1), namely, the specification of the constraints system $\varphi(p^{\nu})$, set of permissible alternatives, information uncertainty, etc. Let us consider some of the results of the risk assessment of PHA with full-gauged stabilizers for flat calculation scheme [5, 7] and conditions of angle maintain, dynamic stability.

For the wellbore angle maintenance condition, bit side force F_B limitation will be used:

$$(F_B)^2 - [F_B]^2 \le 0 \tag{2}$$

where $[F_B]$ is the permissible value of bit side force. The fulfillment of dynamic stability condition for lateral vibrations which are generated by bit operation is given in the form of [5, 7]:

$$\left|\frac{a_{DC}}{a_B}\right| \le 1 \tag{3}$$

where a_B, a_{DC} are amplitude of lateral displacements on the bit and at the random BHA coordinate from the bit to the contact point DC with wellbore wall respectively and $a_{DC} = a_B$ only on the bit.

It should be noted that the static characteristics should include the limitation of stabilizer reactions and contact point DC with wellbore wall [2–5, 7]. Condition (3) determines BHA ability to damp lateral vibrations which are generated by the drill bit on the borehole bottom. This has a positive effect on drill bit performance.

Risk analysis of PHAs, designed according algorithm [10] for rotary drilling of vertical and inclined sections by three-cone and PDC bits in order to minimize bit side force and provide dynamic stability (3), was carried out taking into account an influence of different factors (angle, drilling practice, presence of local caverns, etc.) both separately and in combination. The latter used the methods of numerical experiments planning.

In Monte Carlo methods, the simulation of continuous random variables was performed as statistically independent for normal or uniform laws of probability distribution. The presence of local caverns was modeled as a discrete random variable with a uniform distribution of probabilities.

BHA risks were estimated for conditions (2) and (3) (according r_s and r_d), and their conjunction $r_s \wedge r_d$ and disjunction $r_s \vee r_d$. This information is useful for decision making. The calculation was performed using ANSYS Mechanical APDL [12] and software [5].

The analysis of the research results shows that information uncertainty has a significant impact on the BHA risk indicators. The increase in the power of uncertainty intervals contributes to a rise in risk indicators. The risk of a violation of wellbore angle maintenance (2) is significantly influenced by angle α and weight on the bit *G* while the conditions of BHA dynamic stability (3) are influenced by angle and bit rotation frequency.

Stabilizers in models for the evaluation of characteristics are presented in the form of point support with their fixed location (in the center of the support). Obviously, this inadequately describes the interaction of stabilizers with the wellbore wall. Structural features of stabilizers, in conjunction with local wellbore defects, admit the uncertainty in the traditional task of evaluating static and dynamic BHA characteristics in given drilling conditions [9].

The influence of the calibration surface length of stabilizers on the risk indicators of the designed multi-supported PHA for drilling of inclined sections has been studied. It was found that increasing the calibration of the surface length of the first (from the bit) stabilizer leads to an increase in the risk index (due to the violation of the angle maintenance condition), while changes in the calibration of the surface length of the other stabilizers does not have a significant effect on the risk indicators.

During drilling due to wear, there is a decrease in the stabilizer's diameter and an increase in the clearance between the stabilizer and the wellbore wall. This contributes to the longitudinal bending of a drill string bottom and changes its characteristics. The effect of stabilizer wear on the characteristics of designed multi-supported PHA according to model (1) for drilling vertical and inclined well sections has been investigated. Admissible stabilizer wear was constructed to provide the angle maintenance condition (for the first stabilizer from a bit $\delta_1 = 0$). It has been established that permissible wear of stabilizers does not affect the BHA dynamical stability.

Three-cone and PDC bits have different frequencies of perturbing oscillations, so under other identical conditions, BHAs with these bits can differ only in dynamic characteristics.

The presence of local caverns leads to the contact absence of an arbitrary stabilizer with wellbore wall causing changes in the BHA characteristics. In some cases, changes in characteristics can be significant from the point of view of the limitation system implementation (2) and (3).

Risk study and analysis of multi-supported PHAs shows that the assessment of their effectiveness can be based on the static and dynamic characteristics research for specific drilling conditions in accordance with the decision-making model (1).

3. Example of PHA selection

Consider the PHA design for output data: drill bit diameter 295.3 mm; angle α =17°; weight on the bit 170–190 kN; bit rotation frequency ω = 70–90min^{-1}; drilling fluid density 1170 kg/m^3; DC 203 mm (80 mm inner diameter) length l_{DC} = 150 m; stabilizers contact surface length l_k = 600 mm.

To ensure the angle maintenance condition (2), the limit of bit side force is accepted $[F_B]$ = 1.4 kN. PHA must meet the dynamic stability condition (3) for three-cone and PDC bits. Local cavern formations are possible during drilling, therefore BHA must meet (2) and (3) conditions in the case of one (any) stabilizer contact absence with wellbore wall.

Alternative PHAs variants are proposed according to conditions (2) and (3) which include four (*A*), five (*B*) and six (*C*) full-gauged stabilizers. Their geometrical characteristics are shown in Table 1.

Table 1. Geometric characteristics of BHAs

PHA	Coordinates of stabilizers [m]					
	x_1	x_2	x_3	x_4	x_5	x_6
A	2.0	7.0	12.0	22.0	–	–
B	1.3	2.8	11.0	11.0	16.0	–
C	1.3	2.5	5.5	8.5	11.0	14.0

The risk indexes of alternative variants were built by statistical method of inaccurate information. The angle was modeled as a normal random variable with a mathematical expectation of m_α = 17° and mean square

deviation of $\sigma_\alpha = 1°$. The parameters of drilling practice and the coordinates of stabilizer contact points with the wellbore wall were modeled as uniformly distributed random variables in the given range of their changes (for points of contact $x_i \pm l_i/2$). Local caverns were modeled by the absence of one stabilizer contact with the wellbore wall as a uniformly distributed discrete random variable. The number of statistical experiments was 100.

Table 2 presents the results of PHA characteristics and risks: static characteristics – mean ($\overline{F}_B, \overline{R}_i, \overline{L}$) and variances ($\sigma_F^2, \sigma_{Ri}^2, \sigma_L^2$); dynamic characteristics – the boundary values $\max|a_{DC}/a_B|$ for three-cone and PDC bits; risks – index values ($r_s, r_d, r_s \wedge r_d, r_s \vee r_d$) for three-cone and PDC bits.

In Figure 1, PHA static and dynamic characteristics for three-cone bits are shown with 4 and 5 stabilizers (one of which does not have contact with the wellbore wall) based on statistical simulation results.

Static characteristics reflect the elastic axis shape (ratio of lateral displacement to radial clearance between DC and wellbore wall) from bit to contact point DC with wellbore wall and bit side force, reaction on stabilizers (see Fig. 1a, c)

Dynamic characteristics reflect the distribution of ratios of lateral displacement amplitude for drill string bottom (see Fig. 1b, d). Thus, in particular, for the numerical experiment data in Figure 1b PHA is dynamically unstable (increases the lateral vibrations that are generated by drill bit performance on the bottom hole), and for the data in Figure 1d PHA is dynamically stable (reduces lateral vibrations that are generated by the bit).

Table 2. Assessments of characteristics and risks of BHA

Indexes	BHA		
	A	*B*	*C*
Static characteristics			
$\overline{F}_B / \sigma_F^2$, kN / kN^2	1.37 / 0.942	0.87 / 0.186	0.20 / 0.024
$\overline{R}_1 / \sigma_{R1}^2$, kN / kN^2	4.60 / 7.088	2.80 / 2.982	1.53 / 0.416
$\overline{R}_2 / \sigma_{R2}^2$, kN / kN^2	6.00 / 4.663	6.27 / 15.309	1.54 / 0.618
$\overline{R}_3 / \sigma_{R3}^2$, kN / kN^2	5.59 / 49.598	7.07 / 9.694	4.02 / 10.115
$\overline{R}_4 / \sigma_{R4}^2$, kN / kN^2	13.65 / 0.359	10.31 / 18.562	11.86 / 34.291
$\overline{R}_5 / \sigma_{R5}^2$, kN / kN^2	–	16.75 / 3.121	20.36 / 16.887
$\overline{R}_6 / \sigma_{R6}^2$, kN / kN^2	–	–	22.02 / 8.788
$\overline{L} / \sigma_L^2$, m / m^2	33.97 / 14.816	29.44 / 3.895	28.72 / 1.416
Dynamic characteristics			
$\max \lvert a_{DC} / a_B \rvert$	1.0–37.1 /1.0–11.3	1.0–12.7 / 1.0	1.0 / 1.0
Risks			
r_s	0.39	0.09	0
r_d	0.34 / 0.14	0.07 / 0	0 / 0
$r_s \wedge r_d$	0.22 / 0.01	0.02 / 0	0 / 0
$r_s \vee r_d$	0.52 / 0.53	0.14 / 0.09	0 / 0

Note: For dynamic characteristics and risk indicators, the numerator indicates the use of three cone bits, and the denominator – the PDC bits

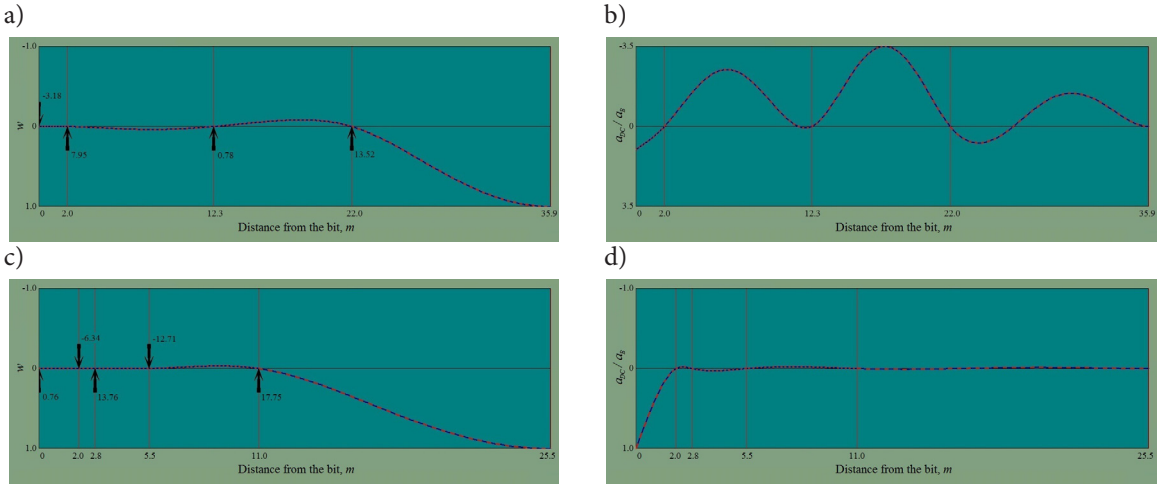

Fig. 1. PHA static (*a, c*) and dynamic (*b, d*) characteristics for three-cone bits with four (*a, b*) and five stabilizers (*c, d*): *a, b* – second stabilizer does not have contact with the wellbore wall (G = 174 kN; ω = 76.8 min^{-1}; α = 17.2 deg); *c, d* – fifth stabilizer does not have contact with the wellbore wall (G = 173 kN; ω = 75.1 min^{-1}; α = 16.8 deg)

Modeling of the results of the analysis of characteristics shows that for PHAs with a greater number of stabilizers, the values dispersion indicators of static characteristics and upper boundaries of dynamic indices are reduced. In particular, PHA *B* with PDC bits and *C* with three-cone and PDC bits are dynamically stable.

The simulation results (see Tab. 2) point to high risk ratios for variant *A* using a three-cone bit ($r_s = 0.39$, $r_d = 0.34$, $r_s \wedge r_d = 0.22$, $r_s \vee r_d = 0.52$), which indicates the inappropriateness of using this PHA. It should be noted that the risk indicator for PDC bits is somewhat lower ($r_d = 0.14$), but the risk indicators combination for conditions of wellbore angle maintenance and dynamic stability ($r_s \vee r_d = 0.53$) is similar to three-cone bits.

Variant *B* is characterized by low risk ratios, and for variant *C*, the risk indicators are zero. It is obvious that these variants can be recommended for use.

Based on the results of statistical simulations, point diagrams of wellbore angle maintenance are shown in Figure 2a, c, e) and dynamic stability (Fig. 2b, d, f) for alternative PHA variants in coordinates angle – weight on the bit and angle – drill bit rotation frequency.

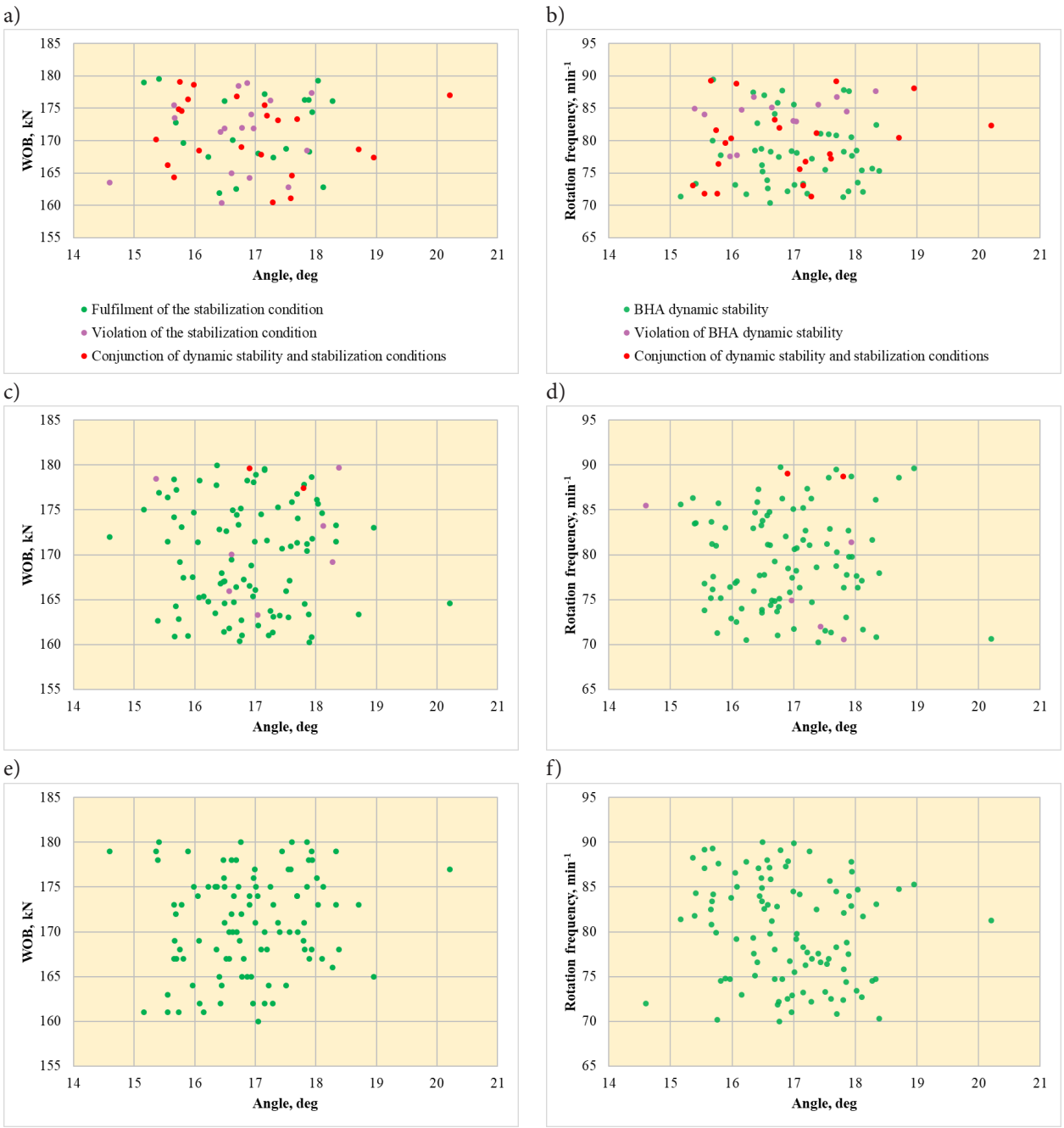

Fig. 2. Diagrams of angle maintenance (a, c, e) and dynamic stability conditions of PHA (b, d, f) with four (a, b), five (c, d) and six (e, f) stabilizers

Diagrams illustrate the distribution of risk indicators for PHA variants due to information uncertainty for three-cone bits.

4. Conclusions

Based on field data about wells quality, a statistical model for PHA design in conditions of information uncertainty (angle, drilling practice parameters, contact point of stabilizer with wellbore wall, presence of local caverns etc.) was substantiated. An optimal variant search is carried out by statistical simulation in a certain class of multi-supported PHA to minimize the risk in the model (1).

The influence of information uncertainty has been analyzed and the directions for the management of BHA risk indicators has been noted. According to the results of the characteristic statistical simulation of PHA alternative variants, including four, five and six stabilizers, the influence of some factors on the risk indicators for the conditions of wellbore angle maintenance and the dynamic stability of drill string bottom have been shown. The increase in the number of stabilizers and their location according to the model (1) reduces BHA risks.

References

[1] Bulatov A.I.: *The concept of quality of oil and gas wells drilled*. Drilling and Oil, no. 12, 2015, pp. 15–19.
[2] Woods H., Lubinski A.: *Curvature of wells during drilling*. HTII, Moscow 1960.
[3] Griguletsky V.G., Lukyanov V.T.: *Designing the bottom-hole assembly*. Nedra, Moscow 1990.
[4] Chen D.C.K., Wu M.: *Maximizing drilling performance with state-of-the-art BHA program*, [in:] SPE/IADC Drilling Conference. Society of Petroleum Engineers, February 2007.
[5] Myslyuk M.A., Novikov V.D., Ovsiannikov A.S., Liakh V.V., Stefurak R.I.: *Calculation of stabilized bottom hole assemblies*. Oil and Gas Industry, no. 1, 1996, pp. 17–19.
[6] Bailey J.R., Biediger E.A.O., Gupta V., Ertas D., Elks W., Dupriest C.F.E.: *Drilling vibrations modeling and field validation*, [in:] IADC/SPE Drilling Conference. Society of Petroleum Engineers, March 2008.
[7] Myslyuk M.A., Rybchych I.J., Yaremyichuk R.S.: *Wells drilling: Directory*, vol. 3. Interpress LTD, Kyiv 2004.
[8] Myslyuk M.A.: *Risk assessment of decision making in drilling*. Construction of Oil and Gas Wells on Land and Sea, no. 1, 2012, pp. 18–23.
[9] Myslyuk M.A., Dolyk R.M.: *Technological decision-making when drilling wells inclined sections*. Construction of Oil and Gas Wells on Land and Sea, no. 4, 2016, pp. 4–13.
[10] Myslyuk M.A., Stefurak R.I., Rybchych I.J., Vasylyuk Yu.M.: *Improving technology of three cone bit run for rotary drilling of wells*. OAO „VNIIOENG", Moscow.
[11] Amorim D., Hanley C., Leite D.J.: *BHA selection and parameter definition using vibration predictions of tware leads to significant drilling performance improvements*, [in:] *SPE Latin America and Caribbean Petroleum Engineering Conference*. Mexico City, April 2012, Paper Number: SPE-152231-MS, https://doi.org/10.2118/152231-MS.
[12] ANSYS Academic Research Mechanical APDL, Release 18.2.